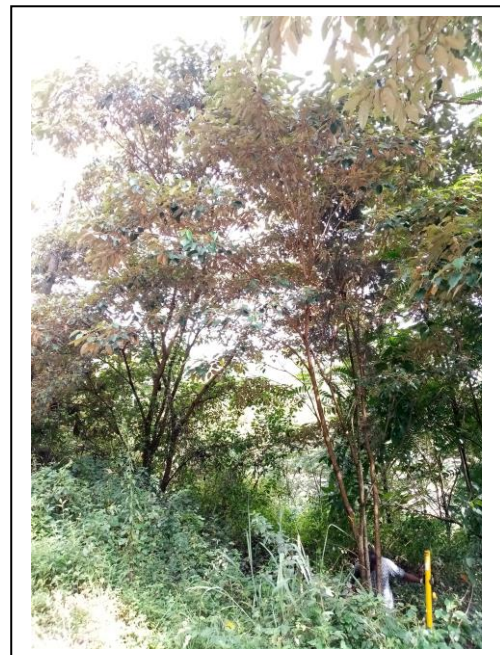




DEPARTMENT OF BIOLOGICAL AND
ENVIRONMENTAL SCIENCES

ALLOMETRIC MODELS FOR ABOVEGROUND BIOMASS IN SMALL AND MULTI-STEMMED TREES IN RWANDA



Carl Svensson

Degree project for Master of Science (120 hec) with a major in Biology
BIO717, Degree project in Evolutionary and Behavioral Ecology (60 hec)
Second cycle

Semester/year: Autumn 2024

Supervisor: Göran Wallin

Examiner: Håkan Pleijel

Sampling process (own picture)

Index (table of contents)

| | |
|---|----|
| Abstract | 2 |
| Sammanfattning | 2 |
| 1. Introduction | 3 |
| 1.1. Background..... | 3 |
| 1.2 Aim..... | 5 |
| 2 Material and method | 6 |
| 2.1. Sample and site..... | 6 |
| 2.2. Measurements of predictor variables..... | 6 |
| 2.3. AGB measurement | 7 |
| 2.4. Statistical analysis | 8 |
| 2.4.1. Estimating AGB..... | 8 |
| 2.4.2. Model structure | 9 |
| 2.4.3. Model selection..... | 10 |
| 2.4.4. Model comparison | 11 |
| 3. Results | 12 |
| 3.1. Model selection | 12 |
| 3.1.1. All samples | 13 |
| 3.1.2. Single-/multi-stemmed subsets | 16 |
| 3.1.3. Species-specific models | 19 |
| 3.2. Model comparison | 24 |
| 3.2.1. Models of this study..... | 24 |
| 3.2.2. Literature models | 27 |
| 4. Discussion | 30 |
| 4.1. Models of this study | 30 |
| 4.2. Models from literature | 32 |
| 4.3. Conclusion..... | 32 |
| References | 32 |
| Appendix | 39 |
| Popular science summary | 39 |
| Supplemental figures and tables | 40 |

Abstract

Estimates of aboveground biomass (AGB) of trees are crucial for understanding how forest ecosystems influence the global carbon cycle and tropical forests are of particular importance. Allometric equations are used to estimate AGB but the allometric relationship differs between sites, species and size of the trees. Most developed equations focus on large trees with one dominant stem. This study focuses on estimating AGB in a population of small and multi-stemmed trees from species native to Rwanda. It aims to test the validity of available equations developed for larger trees and to develop new equations for accurate AGB estimates. Additional measurements of multiple stem diameter, stem count and crown area are tested. A total of 83 trees from 8 species were harvested, and their AGB was measured. The samples' diameter at breast height ranged from 1.6–13.4 cm and 16 samples had multiple stems. Wood density, height, all diameters at 1.3 m and 0.3 m above ground and crown area were measured. AGB was compared to the estimates derived from several equations reported in the literature. New equations were developed through regression analysis. The results show that a commonly used pantropical equation also is valid for the smaller trees of this study. This equation performed almost as good as the model developed in this study, when using the same variables. Moreover, the equation, as well as the simplest equation of this study, is biased regarding trees with different number of stems. Additional measurements of multiple stem diameter or two measurements of the main stem, at different heights, as well as a stem count largely improves the estimates, in particular for multi-stemmed samples. Crown area also improves the estimates. New site- and species-specific equations are presented in this study.

Sammanfattning

Uppskattning av trädets biomassa ovan jord (aboveground biomass, AGB) är avgörande för att förstå hur skogar påverkar den globala kolcykeln där tropiska skogar är av särskild vikt. Allometriska ekvationer används för att uppskatta AGB, men de allometriska förhållandena varierar mellan lokaler, arter och storleken på träd. De flesta ekvationerna som utvecklats fokuserar på stora träd med en dominerande stam. Denna studie fokuserar på att uppskatta AGB för en population små, flerstammiga träd från några inhemska arter i Rwanda. Den ämnar testa validiteten på tillgängliga ekvationer samt att utveckla nya mer precisa ekvationer. Fler variabler, så som flera diametermätningar, stamantal och kronarea testas. Totalt 83 träd från 8 arter skördades, varefter deras AGB mättes. Diametern vid brösthöjd spann mellan 1,6–13,4 cm, 16 flerstammiga träd skördades. Trädensitet, höjd, alla diametrar vid 1,3 m och 0,3 m ovan mark mättes liksom kronarea. AGB jämfördes med estimaten från flera tillgängliga ekvationer. Nya ekvationer utvecklades via regressionsanalys. Resultatet visar att en ekvation ofta använd för tropiska träd även är giltig för träden i denna studie och presterade nästan lika bra som ekvationen utvecklad, när samma variabler användes. Vidare visade dessa två ekvationer samma tendenser till partiskhet beträffande trädets flerstammighet. Tillägg av flertalet diametermått eller två mått av huvudstammen vid olika höjd, liksom stamantal som variabler ökar estimatets tillförlitlighet markant. Även kronarea gav bättre estimat. Ny plats- och artspecifika ekvationer presenteras i denna studie.

1. Introduction

1.1. Background

Forest ecosystems play an important role in the global carbon cycle and tropical forests are of particular importance (Friedlingstein et al., 2020; Pan et al., 2024). At the same time, there is a large uncertainty regarding the future of this biome (Clark et al., 2004; Lewis et al., 2009; da Costa et al., 2010; Brienen et al., 2015; Doughty et al., 2023). Estimates of carbon stock and net primary production of forests are largely based on the aboveground biomass (AGB) of trees (e.g., Rappaport et al., 2018; Clark and Clark, 2000). The direct measurement of AGB is costly and destructive. Instead, an estimation based on allometric relationship between mass and other, more easily measured variables, is used (e.g., Mitchard, 2018; Brown et al., 1989).

A common scaling relationship of mass and other dimensions of trees can be assumed through arguments of mechanical and physiological constraints on the plant (King, 1986; Enquist et al., 1998; West et al., 2009). A general rule of relative growth as a power equation and the usage of logarithmic transformation for analysis was described by Huxley as early as 1932. Overman (1994) shows that the AGB is to a great extent a power function of the stem diameter at breast height (DBH). Stochastic variation in AGB relative to tree size makes biological sense (Mascaro et al., 2011). To fulfill the assumption of a linear regression analysis by the method of ordinary least squares (OLS) of linearity and homoscedasticity in the data log-log transformation can be applied (Asuero and Buneo, 2011; Pek et al., 2017). The back-transformed fitted estimates can then be biologically interpreted as the power-law relationship.

However, back-transformation introduces bias in the result due to the nature of the logarithmic mean relating to the median in true scale (Miller, 1984). Several correction factors have been suggested (Clifford et al., 2013), among which the one suggested by Baskerville (1972) is the most used. Baskerville shows a consistent underestimation (10–20%) of biomass estimates using logarithmic regression which can be compensated for with the addition of the estimated variance of the data. The practice of developing allometric equations to estimate AGB through regression analysis of log-log transformed data, with the correction suggested by Baskerville (1972) is widely used (e.g., Ter-Mikaelian and Korzukhin, 1997; Cole and Ewel, 2006; Ali et al. 2015; Chave et al., 2005 and 2014).

Although trees, as argued above, should assume a similar scaling to maximize the usage of available resources, environmental factors and trade-off between different resources cause variation in tree architecture. Anderson-Teixeira et al. (2015) show that many traits of a tree are logarithmically linear to stem diameter, but the slope of the line can differ between species and be affected by environmental factors.

The ratio of height-to-stem diameter varies due to environmental and ecological factors such as geographical location, vegetation structure, precipitation, temperature and altitude (Feldpausch et al., 2011; Nogueira et al., 2008a). King (1996) show differences in crown width and stem diameter in relation to height between species and over the lifetime within species, associated with light access strategies in closed canopy and occasional gaps in a tropical forest of Costa Rica. Variation in wood density is related to species, size, growth rate and water economics (Poorter et al. 2010; King et al., 2005; McCulloh 2012). A fivefold variation between species has been shown within the Amazonian forest, while it was found to be largely taxonomically conserved (Baker et al., 2004). Variation within species and between parts of a tree is related to size and soil properties (Fernside, 1997; Montagu et al., 2005).

Chave et al. (2005) theorize the relationship of AGB to tree volume (obtained from the measurements of stem diameter, height and tapering) and wood density (WD, oven-dried wood mass over fresh volume). The usage of available volume data from forest inventories combined with WD has also been used in AGB estimations (e.g., Bown and Lugo, 1984). Chave et al. (2005)

suggests pantropical allometric equations where the product of the squared DBH, height and WD is used as a single predictor variable, resulting in a conserved unit of mass. The study includes a large dataset of trees from the Neotropics, South-East Asia and Oceania, but no data from the African continent. The structure of the compound variable is valid across sites however, slightly different equations are suggested for dry, moist and wet forests.

The same study shows the order of decreasing importance in giving an accurate estimate of AGB being DBH, WD and height. The choice of predictor variables must balance model simplicity and accuracy (Foster and Sober, 1994), while the necessary measurements must be easy to obtain. DBH is by far the most used predictor variable. WD for all samples is not always possible to obtain but the conservation of WD within taxonomical groups leads to the common practice of using taxonomic or even site means (Ketterings et al., 2001; Chave et al., 2005). The use of WD of individual trees decreases error in the estimate (Fayolle et al., 2013). The usage of site mean could give an accurate stand estimate of AGB but be bias towards some species.

Height is often absent in data from forest inventory and measurements can be highly inaccurate in a closed canopy forest in the tropics (Hunter et al., 2013), therefore many allometric equations exclude this variable (e.g., Chambers et al., 2001; Chave et al., 2001; Fayolle et al., 2013). Since height is related to stem diameter, variation in diameter also explains variation in height to some degree. Large scale variation of height-to-diameter relationship in the tropics exist between continents (with Africa being an intermediate) and on regional scale, while site mean differences is highly related to precipitation patterns and vegetation structure (Banin et al., 2012). From these factors and diameter, height can be estimated (Feldpausch et al., 2011).

Chave et al. (2005) suggest alternative equations for the different forest types without height as predictor variable. These equations increase the error in estimation site AGB (from 12-16% to 19-31%). Fayolle et al. (2013) tested the validity of the moist forest equation on the African continent resulting in an unbiased estimate with only slightly larger variation at tree-level than a local multi-species model (coefficient of variation being 38% compared to 37%). The risk of overestimating AGB in forests dominated by shorter trees are pointed out in Chave et al. (2005) and is well documented in open and transition forests, and at higher altitude (Nogueira et al., 2008a; Nogueira et al., 2008b; Girardin et al., 2010). Instead, local height-to-diameter models can improve the estimate (Marshall et al., 2012).

Later, Chave et al. (2014) suggested yet another solution. A larger and more spread dataset (now also including Africa) supported a single pantropical model with the compound variable of squared DBH, height and WD. The study showed an average error of AGB for a single site being 5% and 50% error for an individual tree. Moreover, a pantropic equation for height estimation was introduced, based merely on environmental factors and DBH. This equation has been shown to perform better than the regional models available in the lowland of central Congo (Kearsley et al., 2017). Incorporated in the AGB equation results in an equation with an environmental variable instead of height. This equation yields a higher error (average site bias 10% and average error 72% on individual trees) but still performs better than the forest type specific equations developed by Chave et al. (2005).

From above mentioned example, it is clear that a large proportion of variance between trees will cancel out in the scale of stand total AGB. The bulk of studies referred to above focus on global and regional carbon budgets of forests. On a smaller scale, variation in height-to-diameter relationship will affect the accuracy of an AGB estimate. Local models of estimating height by DBH perform better than the pantropical model (Kearsley et al., 2017; Scaranello, et al., 2012). Even more is explained by species affiliation than site and environment, while intraspecific variation also occurs related to size (Mugasha and Bollandssås, 2013; Rozendaal et al., 2015, Thomas et al., 2015; Chenge, 2021). Light demand and maximum height are highly correlated with tree architecture. At an early stage of life vertical growth is important and even multi-special correlation of height-to-diameter-ratio to sizes occur, but understory species tend to be shorter than

large species at a given diameter (Poorter et al. 2006). Local environment variation such as wind exposure and canopy openness also cause intraspecific variation (King, 1986 and 1996).

Crown variation is rarely regarded in allometric models. Holding a large proportion of AGB in a tropical forest, size and shape affect the sum (Malhi et al., 2011; Goodman et al., 2014). The rule of common scaling relationship is applicable and crown dimensions of tropical trees correlate with both height and stem diameter, while forest openness and productivity as well as taxonomy plays a role (Shenkin et al., 2020). Poorter et al. (2006) show that 51–98% of the variation within species in crown area (CA) can be explained by height. The difference in strategies of light demanding and shade tolerant species is reflected in differences in branching point and crown dimensions.

Trees with very low first branching point can be regarded as multi-stemmed. A selection of different diameters could be measured. A single measurement at a lower level or just below first branching point as well as the squared sum of the diameter of several stems have been suggested. Both CA and tree height correlate with these measurements and with the multiple stem diameters to a higher degree (Magarik et al., 2020).

The AGB of shrubby plants is mostly associated to their CA (Conti et al., 2013). Ali et al. (2015) developed allometric equations for shrubs and small trees from the understory layer of a subtropical forest in China, using crown shape, crown area, and diameter of the longest stem in addition to height and WD. Stem diameter and height proved to be the best predictors in most cases, however CA in combination with diameter and/or height performed best for some individual species.

Hence, the accuracy of an equation is dependent on the allometric variation among the trees and a single predictor variable might not be adequate to describe the variation of AGB. A wider range of trees would lead to greater trade-off between simplicity and accuracy. For a single species or even closely related species DBH could be sufficient to give a very accurate estimate (e.g., Cole and Ewel, 2006; Burrow et al., 2000), while the addition of WD improves the estimate of several species at one or similar sites (e.g., Brown et al., 1995; Deans, et al., 1996; Abich et al., 2022). When the environmental or intra- and interspecific variation increases height or CA might be needed. If the variation is too large, one equation covering all sample might not be applicable.

Small trees have little influence on total AGB of mature tropical forests (Chave et al. 2003; DeWalt and Chave, 2004) and are often ignored in total AGB estimates (but see Lima et al., 2012 and Chave et al., 2003). Allometric equations are in general based on samples with DBH ≥ 10 cm (but see Litton and Kauffman, 2008; Mascaro and Schnitzer, 2011). Allometric relationships can vary with size (Cole and Ewel, 2006) and equations cannot be assumed to be accurate outside their size range (Clark et al, 2001; Chave et al., 2004).

Small trees can however hold more biomass in other forest types and regions (Murphy and Lugo, 1986; Clark et al., 2001; Memiaghe et al., 2016). Furthermore, AGB and net primary production in small trees can be of importance in field experiments (e.g., Ntirugulirwa et al., 2023). Ntirugulirwa et al. (2023) investigate tree growth in response to climate in young mixed-species plantations. In lack of reliable allometric equations growth measurements are restricted to diameter and height increasement. Accuracy on individual tree-level is of importance but due to the possible variation in tree allometry in the samples, important information on productivity and carbon assimilation could be lost.

1.2 Aim

The aim of this study is to enable accurate AGB estimates of the target trees at the experimental sites used in Ntirugulirwa et al. (2023). The validity of several equations available in the literature will be tested. New site- and species-specific equations will be developed and assessed for the selection of suitable equations of known accuracy. Moreover, due to the tendency of some species to assume a multi-stemmed architecture some more unorthodox predictor variables are tested. The questions I aim to answer in this thesis are as follows:

1. How accurate are the available equations in estimating the AGB of the trees in the experimental plantation?
2. Which equation describes the relationship of AGB and possible predictor variables best? Here, both accuracy and practicality will be addressed.
3. Will measurement of CA, additional stem diameter measurements and stem count improve the accuracy of the models?

2 Material and method

2.1. Sample and site

Trees were sampled in three locations in Rwanda: Rubona (2°28'44"S, 29°46'19" E), Arboretum de Ruhunde (2°36'48"S, 29°45'16"E) at the altitude of 1 600 m asl and 1 640 m asl, respectively and Sigira (2°3'54" S, 29°23'44"E) at the altitude of 2 400 m asl, in two sampling campaigns, by two sampling teams in February–March, and April 2020.

The selection of samples was conducted so that at least 10 samples per species were obtained, fitting the size range (in height) of the aim (see Table 1). For multi-stemmed species, samples with different number of stems were selected. The selection of trees sought to obtain an as even distribution of size and number of stems across the size range as possible. When possible, an evenly distributed variation of canopy openness and understory type was also sought among the samples. The sampled species with multi-stemmed samples were *Bridelia micrantha*, *Croton megalocarpus*, *Macaranga kilimandscharica* and *Polyscias fulva*; and the single-stemmed species were *Entandophragma excelsum*, *Markhamia platycalyx*, *Newtonia buchananii* and *Podocarpus falcatus*. Trees where growth was affected by injuries were discarded. Due to the destructive method of data collection the selection of samples was limited by permission to cut down the trees in certain areas and the abundance of trees fitting the aim in these areas.

Table 1. Summary of collected samples. S-S. is single-stemmed and M-S. is multi-stemmed.

| | No. Species | No. Samples | No. M-S. Samples |
|--------------|-------------|-------------|------------------|
| Total | 8 | 83 | 16 |
| S-S. Species | 4 | 43 | 0 |
| M-S. Species | 4 | 40 | 16 |

| | Height Range (cm) | No. Stems Range |
|--------------|-------------------|-----------------|
| Total | 138–1097 | 1–7 |
| S-S. Species | 179–1097 | 1 |
| M-S. Species | 138–987 | 1–7 |

2.2. Measurements of predictor variables

Prior to harvesting the trees, several measurements were taken for each individual. Height of tree in cm was measured with a graduated pole. Stem diameter in mm was measured at two levels, 0.3 m and 1.3 m above ground with a caliper. For all stems with a diameter ≥ 15 mm, measurements were taken as the average of two perpendicular measurements at each height. Additionally, the number of stems – with a diameter ≥ 15 mm – was counted at 0.3 m above ground. Crown area was determined by two perpendicular measurements of the horizontal diameter of the crown in cm (first measurement being at approximately the widest). Mean of the two measurement was then used to calculate the crown area (cm²), assuming circular shape. An illustration of the collected measurements is shown in Figure 1.

An initial estimation of stem diameter was done with tools, specifically made for this purpose, working as calipers set at fixed widths (15, 30 and 50 mm), determining if stem diameter was less than fixed widths. These tools were used to determine which diameters to measure and also to group subsamples into different stems and compartments.

Mean wood density for each species was determined in g/cm^3 from aliquots representative for the part with a diameter ≥ 30 mm for 4–10 samples per species, as the ratio of below bark dry mass (see below) and fresh volume of the aliquots, measured either with displacement method or (if too large) calculated from length measurements.

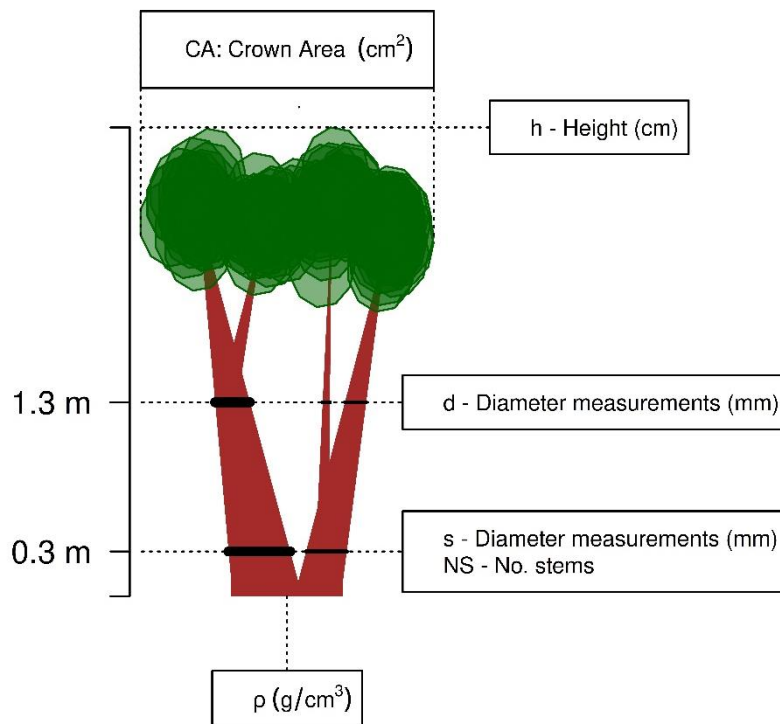


Figure 1. An illustration of the measurements taken, used as predictor variables. Thicker black lines indicate which diameter measurements would be used as "main stem" diameter.

2.3. AGB measurement

The method of measuring AGB follows the procedure described by Picard et al. (2012).

Sample trees were harvested by cutting them as close to the ground as possible (1–5 cm). Samples were measured immediately after harvest, to minimize water loss before measurements. The tree was divided into compartments based on assumed difference in water content (diameter ≥ 50 mm, 50–30 mm, 30–15 mm and < 15 mm, including leaves and fruits). The largest compartments were divided into logs with a length of 2 m (or 1 m for smaller samples). If branching occurred, logs were separated at branching point. Fresh mass of the separate compartments and logs was measured in field before aliquots were taken for further measurements in the lab.

For the tree compartments including leaves and fruits, one or more branches were taken and divided into twigs, leaves and fruit, which were weighed and packed separately. For species *E. excelsum* and *P. fulva* (due to their architecture with composed leaves mounted directly on thicker branches) this compartment was only leaves, which was divided into leaflet (treated as leaves) and petiole (treated as twigs). For these species, an additional compartment was made up of the top of the

branch, starting just below the first leaf. For logs a wooden disk of approximately 3 cm width was taken at each cutting point. In cases where disks were too large for laboratory measurements (see below), they were divided into a half or quarter, circular sector wise. For other compartments aliquots were made up of at least 5 pieces about 10 cm long covering the range of the compartments. All aliquots were packed in paper bags and weighed before transported to the laboratory the same day.

Aliquots were dried in an oven at 70° C. Drying aliquots were weighed repeatedly and regarded as dry when no further weight loss was detected. Dry mass measurements were taken within 2 hours of removal from the oven, to minimize absorption of air humidity. The dry mass of the entire compartments was estimated using the dry-to-fresh ratio of the aliquots and then summed to calculate the total AGB of the sample. Total leaf mass was derived from the proportion of leaves in the aliquot.

Mass measurements were taken with several different scales of varied quality. To test if scale usages would affect the result, measurements of the same object with different scales were performed with no significant difference. Some samples were packed in paper bags prior to weighing. All paper bags used were of the same type (two sizes), which enabled a mean of 50 bags per size to be used to adjust weights when needed.

2.4. Statistical analysis

2.4.1. Estimating AGB

The relationship of AGB and the variables above is commonly assumed to take the form of a power function and can therefore be described in a general form as the following equation:

$$AGB = \alpha \prod x_i^{\beta_i}. \quad (1)$$

After applying the log-log transformation the relationship assumed following linear form:

$$\ln(AGB) = \alpha' + \sum \beta_i \ln(x_i), \quad (2)$$

where $\alpha' = \ln(\alpha)$.

The estimation of $\ln(AGB)$ for each set of x_i is expected to deviate from the true $\ln(AGB)$ with an error of ε , where ε is a random variable with normal distribution around the mean 0 and the variance of σ . An estimate of σ (commonly called the residual standard error, RSE) can be calculated from the residuals ε_i of the regression as follows:

$$\sigma_{est} = \sqrt{\frac{1}{N-p} \sum \varepsilon_i^2}. \quad (3)$$

Although ε is independent from the logarithm of AGB (if assumption of homoscedasticity is true), this is not true for the untransformed AGB . If the true relationship of AGB and the independent variables is as described in Eqn (1) the error term is proportional to AGB (expecting larger error in larger samples). Estimating AGB by simply back-transformation of Eqn (2) will thereby generate an underestimation of up to 10-20% (Baskerville, 1972). Baskerville suggests correction factor ($e^{\sigma^2/2}$), which is commonly use in tree biomass estimations (e.g., Chave et al., 2005, Colgan et al.,

2013, Brown et al., 1989). By estimating the coefficients α' and β_i in Eqn (2), and back-transforming it together with the correction factor, an estimate of AGB can be described as follows:

$$AGB_{est} = e^{\alpha' + \sum(\beta_i \ln(x_i)) + \frac{\sigma^2}{2}} \quad (4)$$

The estimation of α' and β_i is done through multiple regressions (OLS) of the dependent variable (i.e., AGB) and a number of different independent variables (x_i). The independent variables used in the different regressions were stem diameter at 1.3m above ground (d), stem diameter at 0.3m above ground (s), tree height (h), number of stems at 0.3m above ground (NS), crown area (CA) and species-mean wood density (ρ). For d and s several measurements per sample can occur (if several stems ≥ 15 mm). Both the maximum measurements of the sample (denoted simply as d and s , referred to as the main stem diameter) and summations (denoted d_{sum} and s_{sum}) are used. In addition, some combinations and polynomials of above-mentioned variables were used. For a full overview of the variables in transformed form, see Table 2.

2.4.2. Model structure

To select plausible models to test against the sampled data, a literature search was made for used equations to describe tree above ground biomass, with focus on regions and forest type similar to the study site as well as trees with multiple stems (Chave et al., 2005 and 2014; Ali et al., 2015; Magarik et al., 2020). A presentation of predictor variable combinations for models is shown in Table 3. Most variables are divided into three categories. Category 1 contains only the maximum diameter at breast height (d) and different polynomial forms of it. Category 2 contains additional diameter measurements such as the maximum diameter at 0.3 m (s) and the sum of diameters at different heights of first and second dimension. Category 3 contains the remaining variables, height (h), crown area (CA) and stem count (NS) separately and in combination. With the limitation of maximum 5 variables per model, all possible combinations selecting one row from each category or one from either category 1 or 2 and one from category 3 are tested. Moreover, the variable ρ is added to these models when tested on data including more than one species. In addition, compound variables of the product of d^2 , h with and without ρ ($d^2h\rho$ and d^2h) is combined with each row of category 3. In total 113 models are hence constructed. To separate the models in the following text models are named and referred to by the combination of variable symbols (see Table 2) where dots indicate separate variables in the model.

Table 2. Variables used for regression analysis. Diameters are in mm, height in cm, CA in cm² and ρ in g/cm³.

| Symbol | Formula | Comment |
|-------------|-------------------|--|
| CA | $\ln(CA)$ | where CA is the crown area ($r^2\pi$). |
| h | $\ln(h)$ | where h is the height of the tree. |
| d | $\ln(d)$ | where d is the largest diameter at 1.3 m. |
| d^2 | $(\ln(d))^2$ | where d is the largest diameter at 1.3 m. |
| d^3 | $(\ln(d))^3$ | where d is the largest diameter at 1.3 m. |
| d_{sum} | $\ln(\sum d_i)$ | where d_i is all diameters > 15 mm at 1.3 m. |
| d_{sum}^2 | $\ln(\sum d_i^2)$ | where d_i is all diameters > 15 mm at 1.3 m. |
| d^2h | $\ln(d^2h)$ | where d is the largest diameter at 1.3 m and h is the height of the tree. |
| $d^2h\rho$ | $\ln(d^2h\rho)$ | where d is the largest diameter at 1.3 m, h is the height of the tree and ρ is mean SWD of the species. |
| s | $\ln(s)$ | where s is the largest diameter at 0.3 m. |
| s^2 | $(\ln(s))^2$ | where s is the largest diameter at 0.3 m. |
| s_{sum} | $\ln(\sum s_i)$ | where s_i is all diameters > 15 mm at 0.3 m. |
| s_{sum}^2 | $\ln(\sum s_i^2)$ | where s_i is all diameters > 15 mm at 0.3 m. |
| NS | $\ln(NS)$ | where NS is number of stems with an diameter > 15 mm at 0.3 m. |
| ρ | $\ln(\rho)$ | where ρ is mean SWD of the species. |
| AGB | $\ln(AGB)$ | where AGB is the total Aboveground biomass. |

Table 3. Overview of how predictor variables are combined for regression analysis, referring to the symbol of transformed variables (see Table 2). Variables from each box are combined with variables in adjacent box, accumulative from left to right.

| | Category 1 | Category 2 | Category 3 |
|--------|--|--|--|
| ρ | d d^2 $d + d^2$ $d + d^2 + d^3$ | d_{sum} d_{sum}^2 s s^2 s_{sum} s_{sum}^2 | h CA NS $h + CA$ $h + NS$ $NS + CA$ |
| | d^2h $d^2h\rho$ | | |

2.4.3. Model selection

The models were fitted to all samples as well as subsets for individual species, single-/multi-stemmed species and single-/multi-stemmed individuals. When all data points of a variable were equal within a testing-group (i.e. ρ in single species, NS in single-stemmed groups) this variable was removed from the model. For models with multiple independent variables their reduced forms were also tested individually, removing variables one at a time (from right to left). To evaluate if additional variables made the model significantly different from the reduced forms ANOVA-

comparisons were performed on models of interest. To assess the goodness of fit for each model the Akaike information criterion (AIC) and coefficient of determination (adjusted R² for models with multiple variables, hereon referred to as R²) was calculated. Lowest AIC was used as the main indicator of best performing model after discarding models with non-significant coefficients. The practicality of the model (i.e. labor demand for data collection) was also taken into account and best models were selected for each level of practical applicability, levels being *all models*, *main stem* (excluding measurements on multiple stems), *main stem, no CA* (excluding multiple stems and CA), *main stem, no NS* (excluding multiple stems and stem count) and *basic models* (only including ρ , d and h measurements). One equation for every dataset and model category was selected. The variance distribution of selected models was tested with a Breusch-Pagan test to detect heteroscedasticity in the models.

2.4.4. Model comparison

In addition to AIC and R², a bias estimate and a coefficient of variation (CV) was calculated to determine whether a model fitted on multiple species or multi-stemmed and single-stemmed individuals was biased to any group and if the relative deviation varied among groups. The measure of model bias comparing different sites in Chave et al. (2005) was here used to compare different groups and can be described as:

$$Bias_j = \frac{\sum AGB_{est,i,j} - \sum AGB_{obs,i,j}}{\sum AGB_{obs,i,j}}, \quad (5)$$

where $Bias_j$ is the model's mean bias for group j and $AGB_{est,i,j}$ and $AGB_{obs,i,j}$ is the estimated (Eqn. 4) and observed AGB for individual i in group j .

As in Chave et al. (2014), AGB_{est} and AGB_{obs} were used to calculate the model residual standard error (not to be confused with the regression RSE, σ_{est}), which was divided by the observed mean AGB to obtain the CV for different groups, as follows:

$$CV_j = \sqrt{\frac{\frac{1}{N_j - p} (\sum AGB_{est,i,j} - \sum AGB_{obs,i,j})^2}{\frac{1}{N_j} \sum AGB_{obs,i,j}}}, \quad (6)$$

where N_j is the sample size of the group and p is the number of estimated parameters in the model.

To test whether equations developed in this study perform better than previously developed equations, a selection of equations in the literature were tested by estimating the biomass of the dataset and calculating the bias and CV of these models. The selection of literature models was based on relevance for the current dataset, regarding region and forest type as well as inclusion of multi-stemmed samples.

Two equations from Chave et al. (2014) were selected, being generic pantropic equation. The compiled data used in this study range from $DBH \geq 5$ cm up to large trees ($AGB > 30$ Mg). Model 1 uses the equation with one compound variable ($d^2 h \rho$). The second equation uses the variables ρ , d and d^2 and an additional parameter accounting for variation in h due to environmental factors. Model 2 is an adjusted form of this equation, adapted to the current dataset by replacing the equations intercept and the environmental factor by a new intercept (k) based on the observed ABG of all samples in this study, d , d^2 and ρ and the coefficients of the equation. The procedure is described in (Eqn. 7):

$$k = \frac{\sum (\ln(AGB_{obs,i}) - (0.976 \ln(\rho_i) + 2.763 \ln(d) - 0.0299 \ln(d)^2))}{N} \quad (7)$$

Model 3 is a pantropical equation developed for moist forests (Chave et al., 2005) with a polynomial of d and ρ as predictor variables, the DBH range of the data uses in the study is 5–156 cm. Model 4 and Model 5 are multi-species models developed on small trees and shrubs in subtropical China (Ali et al., 2015), the former including CA while the latter only including ρ , d and h . The study site was a subtropical evergreen broadleaved forests and the samples were taken from the shrub layer with a maximum height of just over 4 m. The diameter range of the samples was 4-49 mm. A single diameter measurement was taken for every sample, that of the longest stem. The literature models tested are listed below, expressed in cm for diameter measurements, g/cm³ for ρ and m and m² for height and crown area.

$$\ln(AGB_{est}) = -2.699 + 0.975 \rho d^2 h \quad (\text{Model 1})$$

$$\ln(AGB_{est}) = -1.718 + 0.976 \ln(\rho) + 2.673 \ln(d) - 0.0299 \ln(d)^2 \quad (\text{Model 2})$$

$$\ln(AGB_{est}) = -1.499 + \ln(\rho) + 2.148 \ln(d) + 0.207 \ln(d)^2 - 0.0281 \ln(d)^3 \quad (\text{Model 3})$$

$$\ln(AGB_{est}) = -3.89 + 3.23 \ln(\rho) + 1.52 \ln(d) + 0.83 \ln(h) + 0.145 \ln(CA) \quad (\text{Model 4})$$

$$\ln(AGB_{est}) = -4.06 + 3.31 \ln(\rho) + 1.65 \ln(d) + 0.885 \ln(h) \quad (\text{Model 5})$$

All statistical analyses were performed with the R statistical software (R, version 4.4.1).

3. Results

The range of measured diameters of main stem was 16-134 mm at 1.3 m above ground and 21-163 at 0.3 m. Measured AGB range from 138 g to 86 445 g (mean 8 858 g and median 3 255 g). Species-mean wood densities (ρ) were: 0.60 for *B. micrantha*, 0.67 for *C. megalocarpus*, 0.36 for *E. excelsum*, 0.34 for *M. kilimandscharica*, 0.54 for *M. platycalyx*, 0.57 for *N. buchananii*, 0.58 for *P. falcatus* and 0.34 for *P. fulva*.

3.1. Model selection

Only a selection of models is presented. The selection is mainly the best performing models (i.e., lowest AIC) with some additional, related models for comparison. Models' coefficients for each variable (β_x) are regarded as significant if p-value < 0.05 (in ANOVA-tests, comparing model to reduced forms), while all p-values > 0.01 for coefficients improving model performance are reported in the following text. None of the models selected based on AIC showed significant heteroscedasticity in the Breusch-Pagan test. For residual plots of selected models, see Figure A1 in the appendix. For convenience, the logarithmic scale of the variables is assumed and not printed out. Second and third dimension are equal to $(\ln(x))^n$, where n is the dimension. Sums and squared sums are equal to $\ln(\sum x_i)$ and $\ln(\sum x_i^2)$ respectively.

3.1.1. All samples

A summary of the best performing models for all samples is presented in Table 4. The overall best model (i.e. lowest AIC) is Model. $\rho.d^2.s_{sum}.NS$ with an AIC of 12 and a R^2 of 0.97 followed by the similar Model. $\rho.d^2.s_{sum^2}.NS$ (differ only by exchanging the sum of s_i to the squared sum), with only marginally higher AIC and lower R^2 . Extending these models with the variable h or CA impaired their performance. Further reduction to Model. $\rho.d^2.s_{sum^2}$ also exhibits a high performance with an AIC of 17 and R^2 of 0.96. Extending this model with h marginally improves the result but β_h is non-significant. Extending by CA instead impairs the models. Model. $\rho.d^2.s_{sum}$ gives similar results as Model. $\rho.d^2.s_{sum^2}$, with similar pattern for extensions but with about 1–2 higher AIC-values overall. Notable is that an extension with h in this case impairs the model. In order of lowest AIC, following the various models with variables of sum or squared sum of s , are Model. $\rho.d^2.s.NS$ and Model. $\rho.d^2.s^2.NS$ with an AIC of 24 and 25, respectively (R^2 is 0.96 for both). Neither of the models benefits from further extensions. For models using sum or squared sum of d_i Model. $\rho.d^2.d_{sum}.CA$ has the lowest AIC (26) and a R^2 at 0.96. Reducing the model by CA slightly increases AIC (27), but β_{CA} is not significant. Compared to this model similar models with h or NS instead of CA perform worse. All the top performing models mentioned above included the second dimension of d . Models using first dimension of this measurements instead exhibit similar patterns with the exception of around 10–15 higher AIC and no more than 1% decrease of R^2 (results not shown). Extending above mentioned models by using both the first and the second or all three dimensions of d increases AIC in all cases and has no or negative effect on R^2 .

Table 4. Summary of statistical results of the best performing models for all samples, all models included. Asterisks indicate the models with lowest AIC for each box (grouping model by variable similarity).

| | AIC | R^2 | $\hat{\sigma}$ |
|-----------------------------------|------|-------|----------------|
| Model. $\rho.d^2.s_{sum}$ | 17.4 | 0.963 | 0.259 |
| * Model. $\rho.d^2.s_{sum}.NS$ | 11.7 | 0.966 | 0.249 |
| Model. $\rho.d^2.s_{sum}.h.NS$ | 13.0 | 0.965 | 0.250 |
| Model. $\rho.d^2.s_{sum}.CA.NS$ | 13.5 | 0.965 | 0.250 |
| * Model. $\rho.d^2.s_{sum^2}.NS$ | 11.9 | 0.966 | 0.249 |
| Model. $\rho.d^2.s_{sum^2}.h.NS$ | 13.4 | 0.965 | 0.250 |
| Model. $\rho.d^2.s_{sum^2}.CA.NS$ | 13.8 | 0.965 | 0.251 |
| Model. $\rho.d^2.s_{sum^2}$ | 16.6 | 0.963 | 0.258 |
| * Model. $\rho.d^2.s_{sum^2}.h$ | 16.5 | 0.964 | 0.256 |
| Model. $\rho.d^2.s_{sum^2}.CA$ | 18.6 | 0.963 | 0.259 |
| * Model. $\rho.d^2.s_{sum}$ | 17.4 | 0.963 | 0.259 |
| Model. $\rho.d^2.s_{sum}.h$ | 19.4 | 0.962 | 0.261 |
| Model. $\rho.d^2.s_{sum}.CA$ | 19.4 | 0.962 | 0.261 |
| Model. $\rho.d^2.s$ | 70.4 | 0.930 | 0.355 |
| * Model. $\rho.d^2.s.NS$ | 24.0 | 0.960 | 0.268 |
| Model. $\rho.d^2.s^2$ | 69.6 | 0.931 | 0.354 |
| * Model. $\rho.d^2.s^2.NS$ | 24.9 | 0.960 | 0.269 |
| Model. $\rho.d^2.d_{sum}$ | 27.4 | 0.958 | 0.275 |
| * Model. $\rho.d^2.d_{sum}.CA$ | 26.2 | 0.959 | 0.272 |
| Model. $\rho.d^2.d_{sum}.h$ | 29.3 | 0.958 | 0.277 |
| Model. $\rho.d^2.d_{sum}.NS$ | 29.3 | 0.958 | 0.277 |

Excluding sum and squared sum of s_i as a variable reduces model performance. A summary of best performing models in the category *main stem* is shown in Table 5. For all models excluding any diameter measurements on multiple stems Model. $\rho.d^2.s.NS$ and Model. $\rho.d^2.s^2.NS$ has the lowest AIC (even lower than any model with sum or squared sum of d_i), as mentioned above. In order of lowest AIC followed similar models with the first dimension of d instead of the second, with similar

patterns for extensions. Following the models with variables d and s (in first or second dimension) extended with NS or CA , Model. $\rho.d^2.CA.NS$ has the lowest AIC in this category (53, with a R^2 of 0.94). Reducing this model by CA has a small deteriorating effect (AIC increased to 56) while reduction by NS has a large negative effect on model performance (increase of AIC to 80). Coefficients of both variables are significant in the full model although β_{CA} is close to the upper limit with a p-value of 0.03. Comparing models with only one diameter measurement, breast height diameter d is preferable before measurements taken at 0.3 m above ground, as demonstrated by Model. $\rho.s^2.CA.NS$ and Model. $\rho.s^2.NS$ (see Table 4). For this category of models NS -inclusion is important for model performance, demonstrated by the lowest found AIC for models excluding this variable is in Model. $\rho.d^2.s^2.CA$ at 66 (R^2 0.93), where the p-value for β_{CA} is 0.03, with no improvement for the extension of h .

Table 5. Summary of statistical results of the best performing models for all samples, in the category *main stem*. Asterisks indicate the models with lowest AIC for each box (grouping model by variable similarity).

| | AIC | R^2 | $\hat{\sigma}$ |
|----------------------------|------|-------|----------------|
| Model. $\rho.d^2.s$ | 70.4 | 0.930 | 0.355 |
| * Model. $\rho.d^2.s.NS$ | 24.0 | 0.960 | 0.268 |
| Model. $\rho.d^2.s.h.NS$ | 26.0 | 0.960 | 0.27 |
| Model. $\rho.d^2.s.CA.NS$ | 26.0 | 0.960 | 0.27 |
| Model. $\rho.d^2.s^2$ | 69.6 | 0.931 | 0.354 |
| * Model. $\rho.d^2.s^2.NS$ | 24.9 | 0.960 | 0.269 |
| * Model. $\rho.d^2.CA.NS$ | 52.6 | 0.944 | 0.318 |
| Model. $\rho.d^2.NS$ | 55.7 | 0.941 | 0.325 |
| Model. $\rho.d^2.CA$ | 79.6 | 0.922 | 0.375 |
| * Model. $\rho.s^2.NS$ | 64.3 | 0.935 | 0.342 |
| Model. $\rho.s^2.CA.NS$ | 64.6 | 0.935 | 0.341 |
| * Model. $\rho.d^2.s^2.CA$ | 66.4 | 0.934 | 0.345 |

Since all top performing models of above-mentioned category also is included in the model category *main stem, no CA* (with the exception of the full model Model. $\rho.d^2.CA.NS$, where the reduced of CA has a small effect on model performance), results for this category are referred to the paragraph above and Table 5. The corresponding category with exclusion of the variable NS (*main stem, no NS*) is summarized in Table 6. The lowest AIC is found in model Model. $\rho.d^2.s^2.CA$ as mentioned above (AIC 66 and R^2 0.93, p-value of 0.03). Extension of h has a marginal increase of AIC, with no significance for the coefficient. Exchanging variable CA with h (Model. $\rho.d^2.s^2.h$) result in a small impairing effect of model performance (increase of AIC from 66 to 68), but β_h is not significant in this model (p-value 0.06). Reducing the model to only diameter measurements have a similar (but higher) performance (AIC 70). Limiting the models to using only one diameter measurement result in the lowest AIC (80) in model Model. $\rho.d^2.CA$ (with R^2 at 0.92). Extension by h impairs the model performance. Comparing the AIC of this model to the AIC of Model. $\rho.d^2.h$ (while exchanging CA with h) at 89 (R^2 0.91) exhibits the improvement of models by including CA as a variable.

Table 6. Summary of statistical results of the best performing models for all samples, in the category main stem, no NS. Asterisks indicate the models with lowest AIC for each box (grouping model by variable similarity).

| | AIC | R ² | $\hat{\sigma}$ |
|----------------------------|------|----------------|----------------|
| Model. $\rho.d^2.s^2$ | 69.6 | 0.931 | 0.354 |
| * Model. $\rho.d^2.s^2.CA$ | 66.4 | 0.934 | 0.345 |
| Model. $\rho.d^2.s^2.h$ | 67.8 | 0.933 | 0.348 |
| Model. $\rho.d^2.s^2.h.CA$ | 66.8 | 0.934 | 0.344 |
| * Model. $\rho.d^2.CA$ | 79.6 | 0.922 | 0.375 |
| Model. $\rho.d^2.h.CA$ | 81.0 | 0.921 | 0.376 |
| Model. $\rho.d^2.h$ | 88.8 | 0.913 | 0.396 |

For models including only the commonly used variables based on the measurements of wood density, DBH and height of the tree (category *basic models*) the lowest AIC is found at 89 in Model. $\rho.d^2.h$. A reduction of this model by h result in a small increase of AIC and decrease of R² but β_h is not significant (p-value of 0.08). For a summary of best performing models in this category, see Table 7. Additional dimensions of d do not improve model performance and using first dimension only result in higher AIC than models including the second dimension, as is shown in the comparison of Model. $\rho.d.h$ to Model. $\rho.d.d^2.h$ and Model. $\rho.d.d^2.d^3$. Highest AIC of all models are found at 136 (R² 0.84) in Model. d^2h where diameter and height is combined in one variable, with a clear improved of this variable by the inclusion of ρ (Model. $d^2h\rho$, AIC 128, R² 0.86). The p-value for including ρ in the models is below 0.0001 for all models presented for all samples.

Table 7. Summary of statistical results of the best performing models for all samples, in the category basic models. Asterisks indicate the models with lowest AIC for each box (grouping model by variable similarity).

| | AIC | R ² | $\hat{\sigma}$ |
|-------------------------|-------|----------------|----------------|
| Model. $\rho.d^2$ | 90 | 0.911 | 0.401 |
| * Model. $\rho.d^2.h$ | 88.8 | 0.913 | 0.396 |
| Model. $\rho.d.h$ | 109.4 | 0.889 | 0.448 |
| * Model. $\rho.d.d^2.h$ | 90.7 | 0.912 | 0.399 |
| Model. $\rho.d.d^2.d^3$ | 93.9 | 0.908 | 0.406 |
| * Model. $d^2h\rho$ | 127.5 | 0.859 | 0.505 |
| Model. d^2h | 136.4 | 0.843 | 0.532 |

A summary of the selected models fitted on the whole dataset in the categories *all models*, *main stem* and *basic models* and their equations is presented in Table 8.

Table 8. Summary of selected models from all samples. “Cat.” is model categories: all models (1), main stem (2) and basic models (3). Below are the equations for estimating AGB for each model.

| Cat. | Variables | AIC | R ² | σ |
|------|-----------------------------|------|----------------|-------|
| 1) | $\rho + d^2 + s_{sum} + NS$ | 11.7 | 0.966 | 0.25 |
| 2) | $\rho + d^2 + s + NS$ | 24.0 | 0.960 | 0.268 |
| 3) | $\rho + d^2$ | 90 | 0.911 | 0.401 |
| | $\rho + d^2 + h$ | 88.8 | 0.913 | 0.396 |

Equation

- 1) $AGB_{est} = \exp(1.3 + 0.8\ln(\rho) + 0.1(\ln(d))^2 + 1.3\ln(\sum s_i) - 0.4\ln(NS) + \sigma^2/2)$
- 2) $AGB_{est} = \exp(1.9 + 0.8\ln(\rho) + 0.2(\ln(d))^2 + 1.1\ln(s) + 0.5\ln(NS) + \sigma^2/2)$
- 3) $AGB_{est} = \exp(4.7 + 0.7\ln(\rho) + 0.3(\ln(d))^2 + \sigma^2/2)$

3.1.2. Single-/multi-stemmed subsets

Fitting the models on a subset of the data excluding species with no multi-stemmed samples generates a slightly different result than for all samples. A summary of best performing models for multi-stemmed species in different categories is presented in Table 9. For the subset Model.ρ.d².s_{sum}.h has the lowest AIC (-3) and a R² of 0.97. Reducing this model by *h* yields a marginal increase of AIC, but β_{*h*} is non-significant (p-value is 0.15). For exclusion of variables based on diameter measurements of multiple stems (category *main stem*) Model.ρ.d².s.h.NS has the lowest AIC at 20 (R² 0.96). Reduction by *h* has a marginal effect on the model and β_{*h*} is not significant (p-value is 0.12). Comparing models in category *Main stem, no NS* demonstrates that the variable *CA* is not benefiting the model performance as the lowest AIC for this category is found in model Model.ρ.d².s (AIC 42, R² 0.93) with a marginal increase of AIC when extended by *CA*. When restricting models to using only one diameter measurement, models with second dimension of *s* performs better than *d* with lowest AIC found in Model.ρ.s².h.NS and Model.ρ.d².h.NS (27, R² 0.95 and 41, R² 0.93, respectively). For model Model.ρ.d².h.NS, β_{*h*} is non-significant (with a p-value of 0.12) and the reduction by *h* yield only a marginal increase of AIC (42). For models in category *Basic models* Model.ρ.d² preforms best with an AIC of 56 (R² 0.90), while extension by *h* impairs model performance. The combination of ρ, *d* and *h* into one compound variable (Model.d²hp), has a comparably low performance with an AIC of 70 and an R² of 0.86.

Table 9. Summary of statistical results of the best performing models for multi-stemmed species. Asterisks indicate the models with lowest AIC for each category.

| | AIC | R ² | $\hat{\sigma}$ | |
|-------------------------|-------------------------------|----------------|----------------|-------|
| <i>All models</i> | | | | |
| | Model. $\rho.d^2.s_{sum^2}$ | -2.6 | 0.978 | 0.218 |
| * | Model. $\rho.d^2.s_{sum^2}.h$ | -3.1 | 0.978 | 0.214 |
| <i>Main stem</i> | | | | |
| * | Model. $\rho.d^2.s.h.NS$ | 20 | 0.962 | 0.283 |
| | Model. $\rho.d^2.s.NS$ | 21.0 | 0.960 | 0.289 |
| | Model. $\rho.s^2.NS$ | 34.9 | 0.943 | 0.348 |
| | Model. $\rho.s^2.h.NS$ | 27.1 | 0.954 | 0.312 |
| | Model. $\rho.d^2.NS$ | 41.8 | 0.932 | 0.379 |
| | Model. $\rho.d^2.h.NS$ | 41.0 | 0.935 | 0.372 |
| <i>Main stem, no NS</i> | | | | |
| * | Model. $\rho.d^2.s$ | 41.8 | 0.932 | 0.380 |
| | Model. $\rho.d^2.s.CA$ | 42.4 | 0.932 | 0.378 |
| <i>Basic model</i> | | | | |
| * | Model. $\rho.d^2$ | 56.4 | 0.900 | 0.461 |
| | Model. $.d^2.h$ | 58.4 | 0.897 | 0.467 |
| | Model. $.d^2.h\rho$ | 69.9 | 0.856 | 0.552 |

A summary of best performing models fitted on a subset of the data with multi-stemmed individuals only is presented in Table 10. For this subset Model. $\rho.d.s_{sum^2}.h.CA$ has the lowest AIC (-1) and an R² of 0.99. Reduction by *CA* impairs the model's AIC to 0 while reduction by *h* yields an AIC of 5. β_{CA} is however non-significant when extending both Model. $\rho.d.s_{sum^2}$ and Model. $d.s_{sum^2}.h$ (with a p-value of 0.11 and 0.16, respectively), while β_h remains significant, but with a relatively high p-value for equivalent ANOVA tests (0.02 in Model. $d.s_{sum^2}.h$). Extensions by *NS* impairs any model including *d* (first or second dimension), sum or squared sum of s_i and *h* or *CA*. Lowest AIC of a model improved by the extension of *NS* is 7 for Model. $\rho.d.s_{sum^2}.NS$. The usage of second dimension of *d* instead of the first has an overall higher AIC with the lowest found in Model. $\rho.d^2.s_{sum^2}.h.CA$ at 1 (R² 0.98). When excluding diameter measurements on multiple stems (model category *main stem*) the lowest AIC is found in Model. $\rho.d.s.h.NS$ at 17 (R² 0.96). Reduction by *NS* and further reduction by *h* has marginal effect on model performance and β_{NS} and β_h is not significant (p-values are 0.26 for β_{NS} in Model. $\rho.d.s.h.NS$ and 0.20 for β_h in Model. $\rho.d.s.h$). Extensions of Model. $\rho.d.s$ by *CA* also yields marginally lower AIC with a non-significant β_{CA} (p-value of 0.19). Regarding models including only one diameter measurement, Model. $d^2.h\rho$ has the lowest AIC at 20, with no improvements for extension by *CA* or *NS*. This model performs better than models with ρ , *d* (first or second dimension) and *h* as separate variables (Model. $\rho.d.h$ and Model. $\rho.d^2.h$), where β_h is non-significant (p-value is 0.10) although the full models have a slightly lowest AIC than models reduced by *h*.

Table 10. Summary of statistical results of the best performing models for multi-stemmed samples. Asterisks indicate the models with lowest AIC for each category.

| | AIC | R ² | $\hat{\sigma}$ |
|---|------|----------------|----------------|
| <i>All models</i> | | | |
| Model. ρ .d. s_{sum^2} .h | 0.2 | 0.984 | 0.202 |
| Model. ρ .d. s_{sum^2} .CA | 4.8 | 0.978 | 0.233 |
| * Model. ρ .d. s_{sum^2} .h.CA | -1 | 0.985 | 0.191 |
| Model. ρ .d. s_{sum^2} .NS | 7 | 0.975 | 0.249 |
| Model. ρ .d ² . s_{sum^2} .h.CA | 0.9 | 0.983 | 0.203 |
| <i>Main stem</i> | | | |
| Model. ρ .d.s | 17.3 | 0.950 | 0.351 |
| Model. ρ .d.s.h | 16.9 | 0.954 | 0.340 |
| * Model. ρ .d.s.h.NS | 16.7 | 0.955 | 0.333 |
| Model. ρ .d.s.NS | 19.2 | 0.946 | 0.366 |
| Model. ρ .d.s.CA | 16.7 | 0.954 | 0.338 |
| <i>Basic models</i> | | | |
| * Model.d ² h ρ | 19.9 | 0.936 | 0.399 |
| Model. ρ .d | 24.3 | 0.920 | 0.446 |
| Model. ρ .d.h | 23.6 | 0.927 | 0.427 |
| Model. ρ .d ² | 25.5 | 0.914 | 0.464 |
| Model. ρ .d ² .h | 24.4 | 0.923 | 0.438 |

For models fitted on a subset of the data with samples of species where no multi-stemmed samples occur, Model. ρ .d² has the overall lowest AIC (-8) and a R² of 0.97. Any extension of this model increases AIC and decreases R². For this model, β_ρ is non-significant (p-value 0.7). Notable is that this subset includes only four species, with smaller variance of ρ than the subset of multi-stemmed species. An additional model with the reduction of ρ was fitted to this subset, yielding lower AIC at -10 (see Table 11).

When including all single stemmed individuals in the dataset, best performing model was Model. ρ .d².s.h with an AIC of -7 and R² of 0.97 (see Table 11). Extension by CA impair model performance as well as the reduced model Model. ρ .d².s. Limiting the models to one diameter measurement yields the lowest AIC (16) in Model. ρ .d².h.CA with a R² of 0.96. Reducing this model by h slightly increases the AIC (to 17) but β_h is non-significant (p-value 0.11), while reduction of CA has a larger negative effect on model performance. This reduced model Model. ρ .d².h, is the best performing model of the category *basic models*, with an AIC at 20 (R² 0.96). Further reduction by h results in an increase of AIC to 24 (p-value for β_h is 0.02). For this subset of data, Model.d²h ρ and Model.d²h has the highest AIC (75 and 84 respectively) with R² of 0.90 and 0.89.

Table 11. Summary of statistical results of the best performing models for single-stemmed species and all single-stemmed samples. Asterisks indicate the models with lowest AIC for each category.

| | AIC | R ² | $\hat{\sigma}$ |
|-------------------------------|-------|----------------|----------------|
| <i>Single-stemmed species</i> | | | |
| Model. $\rho.d^2$ | -8.5 | 0.971 | 0.207 |
| * Model. d^2 | -10.3 | 0.973 | 0.205 |
| <i>Single-stemmed samples</i> | | | |
| Model.. $d^2.s$ | 0.2 | 0.967 | 0.232 |
| * Model.. $d^2.s.h$ | -6.5 | 0.971 | 0.219 |
| Model.. $d^2.s.h.CA$ | -4.7 | 0.970 | 0.221 |
| Model. $\rho.d^2$ | 23.6 | 0.953 | 0.278 |
| * Model. $\rho.d^2.h$ | 19.7 | 0.956 | 0.268 |
| Model. $\rho.d^2.h.CA$ | 16 | 0.959 | 0.259 |
| Model. $\rho.d^2.CA$ | 16.7 | 0.958 | 0.262 |

3.1.3. Species-specific models

A summary of models fitted on samples of species *B. micrantha* is listed in Table 12. The lowest AIC is found in Model.d. s_{sum^2} .NS at -9 and a R² of 0.99. For models in the category *main stem* Model.d².NS performs best with AIC at 5 and R² at 0.94. Slightly poorer performance has Model.d.d².NS (AIC 6), β_{NS} is however not significant in both cases (p-value is 0.14 and 0.46 for Model.d².NS and Model.d.d².NS, respectively). Models with CA perform poorer than their reduced equivalents (e.g., Model.d.d².CA, see Table 12). The best performing model in category *basic models* is Model.d.d² (AIC 5, R² 0.94). Model.d² yields a slightly higher AIC (6) but an ANOVA comparison shows no significant difference from model Model.d.d² with a p-value of 0.17.

Table 12. Summary of statistical results of the best performing models for *B. micrantha*. Asterisks indicate the models with lowest AIC for each category.

| | AIC | R ² | $\hat{\sigma}$ |
|----------------------------|------|----------------|----------------|
| <i>All models</i> | | | |
| Model.d. s_{sum^2} | -6.4 | 0.981 | 0.138 |
| * Model.d. s_{sum^2} .NS | -8.9 | 0.986 | 0.121 |
| <i>Main stem</i> | | | |
| Model.d ² | 6.1 | 0.930 | 0.271 |
| * Model.d ² .NS | 4.7 | 0.943 | 0.246 |
| Model.d.d ² .NS | 6.2 | 0.937 | 0.258 |
| Model.d.d ² .CA | 7 | 0.931 | 0.269 |
| <i>Basic models</i> | | | |
| * Model.d.d ² | 5.2 | 0.940 | 0.251 |
| Model.d ² | 6.1 | 0.938 | 0.272 |

For models fitted on species *C. megalocarpus* best performing model is Model.d.d².d³.NS with an AIC of -3 and R² of 0.99 (see Table 13). Reducing this model by the third dimension of *d* largely increases AIC to 4 although β_{d^3} has a comparably high p-value of 0.04. Models including diameter measurements on multiple stems yield poorer fit, the best being Model.d². s_{sum} .CA with AIC of 3 (R² 0.98). Using basic variables Model.d.d².d³ performs best with an AIC at 9 and R² being 0.97. Reducing this model by the first and third dimension of *d* has a small negative effect on model performance (AIC 10, in both cases) and both coefficients are non-significant compared to the reduced form Model.d² (p-values are 0.17 and 0.20, respectively).

Table 13. Summary of statistical results of the best performing models for *C. megalocarpus*. Asterisks indicate the models with lowest AIC for each category.

| | AIC | R ² | $\hat{\sigma}$ |
|--|------|----------------|----------------|
| <i>All models</i> | | | |
| * Model.d.d ² .d ³ .NS | -3.0 | 0.990 | 0.162 |
| Model.d.d ² .NS | 4.5 | 0.978 | 0.237 |
| Model.d ² .s _{sum} | 5.0 | 0.977 | 0.249 |
| Model.d ² .s _{sum} .CA | 2.6 | 0.982 | 0.216 |
| <i>Basic models</i> | | | |
| * Model.d.d ² .d ³ | 9.1 | 0.967 | 0.298 |
| Model.d.d ² | 10.0 | 0.962 | 0.319 |
| Model.d ² | 10.0 | 0.970 | 0.319 |

For *E. excelsum* the best performing model is Model.d.CV with an AIC of -21 and R² of 0.99 (see Table 14). Reducing this model by CA (to Model.d) yields the lowest AIC for models in category *basic models* (AIC 10, R² 0.97).

Table 14. Summary of statistical results of the best performing models for *E. excelsum*. Asterisks indicate the models with lowest AIC for each category.

| | AIC | R ² | $\hat{\sigma}$ |
|---------------------|------|----------------|----------------|
| <i>All models</i> | | | |
| * Model.d.CA | -21 | 0.9919 | 0.0679 |
| <i>Basic models</i> | | | |
| * Model.d | -9.7 | 0.973 | 0.124 |

Models fitted on samples of *M. kilimandscharica* are summarized in Table 15. Lowest AIC of all models is Model.d².s².h.NS with an AIC of -4 (R² 0.96). Reducing this model by *h* yields a slightly higher AIC (-3, R² 0.95) but β_h is not significant (p-value is 0.24). When restricting models to not using *NS* as a variable, sums or squared sums of multiple stem measurements become important for obtaining a low AIC, lowest being -1 for Model.d².s_{sum}² (which still benefits from further extension by *NS*, lowering AIC to -3). Best performing model with no diameter measurement on multiple stems and no stem count (*NS*) is Model.d².s².CA where reduction of *CA* largely increases the AIC (from 7 to 16). When restricting diameter measurements to *d* Model.d².CA performs best with AIC of 15 (compared to Model.d².NS with AIC of 16). For models in the category *basic models* Model.d²h has the lowest AIC at 22 and a notably low R² of 0.34 and a p-value for β_{d^2h} of 0.045. Marginal higher AIC is found in Model.d with a lower R² (0.30) and a p-value for β_d of 0.057. This model performance poorer when extended with *h*.

Table 15. Summary of statistical results of the best performing models for *M. kilimandscharica*. Asterisks indicate the models with lowest AIC for each category.

| | AIC | R ² | $\hat{\sigma}$ |
|-------------------------|------|----------------|----------------|
| <i>All models</i> | | | |
| | -3.3 | 0.952 | 0.161 |
| * | -4.3 | 0.957 | 0.152 |
| | -1.2 | 0.938 | 0.182 |
| | -2.9 | 0.950 | 0.164 |
| <i>Main stem, no NS</i> | | | |
| | 16.1 | 0.650 | 0.433 |
| * | 7.3 | 0.861 | 0.272 |
| | 14.6 | 0.700 | 0.402 |
| <i>Basic models</i> | | | |
| * | 21.7 | 0.340 | 0.594 |
| | 22.3 | 0.304 | 0.610 |
| | 23.6 | 0.254 | 0.631 |

The best performing model fitted on samples of *M. platycalyx* is presented in Table 16. Lowest AIC is found in Model.s.h.CA at -13 (R^2 0.99). The p-value for β_{CA} is just over the limit of significance (0.05) while the reduction by this variable increases the AIC to -9 , which is the lowest AIC yield without using a non-significant CA in a model. The variable s (in first or second dimension) yields lowest AIC of the diameter measurements, alone as well as in combination of d . The lowest AIC using d as the only diameter measurement is found in Model.d²h.CA at -3 (R^2 0.98), performing better than models with d^2 and h as separate variables (AIC of -1). This model (Model.d².h.CA) exhibits no significant difference from reduced models Model.d² and Model.d².h (p-value of 0.10 and 0.08, respectively). Best performing model in category *basic models* is Model.d²h with an AIC of -1 , compared to Model.d² with an AIC of 1, where the extension by h impairs model performance.

Table 16. Summary of statistical results of the best performing models for *M. platycalyx*. Asterisks indicate the models with lowest AIC for each category.

| | AIC | R ² | $\hat{\sigma}$ |
|----------------------------|-------|----------------|----------------|
| <i>All models</i> | | | |
| Model.s.h | -9.1 | 0.987 | 0.143 |
| * Model.s.h.CA | -12.8 | 0.991 | 0.121 |
| Model.d ² .h.CA | -3.1 | 0.979 | 0.180 |
| Model.d ² .h.CA | -0.6 | 0.976 | 0.194 |
| <i>Basic models</i> | | | |
| * Model.d ² h | -0.8 | 0.973 | 0.203 |
| Model.d ² | 0.7 | 0.970 | 0.214 |
| Model.d ² .h | 1.6 | 0.970 | 0.216 |

For models fitted on samples of *N. buchananii*, lowest AIC is found in Model.d².s².h.CA at -12 (R² 0.99). A summary of these models is presented in Table 17. Limiting models to diameter measurements at breast height yields the lowest AIC at -6 in Model.d².h (R² 0.99), with no improvements by extending it with CA. This model is also the best performing model in category *basic models*. Reduction by *h* impairs the model performance (with an increase of AIC to 2). The model combining these measurements into one variable (Model.d²h) has a poorer performance with an AIC of -4 (R² 0.98).

Table 17. Summary of statistical results of the best performing models for *N. buchananii*. Asterisks indicate the models with lowest AIC for each category.

| | AIC | R ² | $\hat{\sigma}$ |
|--|-------|----------------|----------------|
| <i>All Models</i> | | | |
| Model.d ² .s ² .h | -5.2 | 0.986 | 0.146 |
| * Model.d ² .s ² .h.CA | -12.4 | 0.993 | 0.101 |
| Model.d ² .h.CA | -5.2 | 0.986 | 0.146 |
| <i>Basic models</i> | | | |
| Model.d ² | 1.8 | 0.969 | 0.219 |
| * Model.d ² .h | -6.1 | 0.987 | 0.143 |
| Model.d ² h | -3.7 | 0.982 | 0.166 |

For species *P. falcatus* best fitted model is Model.s² with AIC of -4 (R² 0.99) (see summary in Table 18). When limiting the models to diameter measurements at breast height, Model.d.d².h has the lowest AIC (R² 0.99) with a small increase for the reduction by *h* (from -2 to -1) and further increase for the reduction by the first dimension of *d*. Neither of these reduced models are significantly different for the full model (p-value for Model.d.d².h compared to Model.d.d² is 0.19 and 0.17 for Model.d.d² compared to Model.d²). Extension by *h* to Model.d².h increases AIC (from 0 to 2). In comparison Model.d²h performs poorly with an AIC of 12 and R² of 0.95.

Table 18. Summary of statistical results of the best performing models for *P. falcatus*. Asterisks indicate the models with lowest AIC for each category.

| | AIC | R ² | $\hat{\sigma}$ |
|-----------------------------|------|----------------|----------------|
| <i>All models</i> | | | |
| * Model.s ² | -4.5 | 0.990 | 0.160 |
| <i>Basic models</i> | | | |
| Model.d ² | 0.1 | 0.986 | 0.202 |
| Model.d.d ² | -0.8 | 0.987 | 0.186 |
| * Model.d.d ² .h | -1.9 | 0.989 | 0.172 |
| Model.d ² h | 11.8 | 0.949 | 0.362 |

A summary of best performing models for samples of *P. fulva* is presented in Table 19. Lowest AIC yields Model.d².d_{sum}².CA.NS at -25 (R² is 1), with notably high p-value of 0.04 for β_{NS} . Reducing this model by *NS* increases the AIC to -17. Slightly higher AIC is found in Model.d².d_{sum}.h.CA and the reduced form Model.d².d_{sum}.CA (AIC -24 in both). β_h is non-significant when comparing these two models (with a p-value of 0.29). For models in category *main stem* best performing model is Model.s².CA.NS with AIC of -3. When reducing this model by either of the variables *CA* or *NS* individually AIC increases (to 0 and 2, respectively), while β_{CA} is non-significant and the p-value of β_{NS} is close to the upper limit of significance (0.081 and 0.049, respectively). The remaining coefficients of the reduced models (Model.s².CA and Model.s².NS) are however significant and these models yields the lowest AIC for the categories *main stem, no NS* and *Main stem, no CA*. If limiting models to diameter measurement of main stem at breast height, Model.d².CA.NS has best performance (AIC at 3, R² at 0.98), with no significance for either of the coefficients β_{CA} and β_{NS} , tested separately. For additional limitation of using only one of these variables, Model.d².CA has the lowest AIC (3), while Model.d².h.NS has slightly lower AIC than Model.d².NS (4 and 5, respectively), but with no significance for β_h (p-value is 0.23). For models in the category *basic models* Model.d² has the lowest AIC at 9 (R² at 0.96) performing better than Model.d²h with an AIC of 12 and R² at 0.95.

Table 19. Summary of statistical results of the best performing models for *P. fulva*. Asterisks indicate the models with lowest AIC for each category.

| | AIC | R ² | $\hat{\sigma}$ |
|---------------------|-------|----------------|----------------|
| <i>All models</i> | | | |
| | -17.4 | 0.9976 | 0.0792 |
| * | -25.1 | 0.9989 | 0.0537 |
| | -24.3 | 0.9988 | 0.0558 |
| | -23.9 | 0.9987 | 0.0575 |
| <i>Main stem</i> | | | |
| * | -3.2 | 0.990 | 0.161 |
| | 1.8 | 0.983 | 0.212 |
| | 0.3 | 0.985 | 0.197 |
| | 3.1 | 0.981 | 0.221 |
| | 3.4 | 0.98 | 0.23 |
| | 4.9 | 0.976 | 0.248 |
| | 4.4 | 0.979 | 0.236 |
| <i>Basic models</i> | | | |
| * | 8.6 | 0.963 | 0.309 |
| | 12.4 | 0.947 | 0.373 |

For a summary of all selected models see Table A1 in the appendix.

3.2. Model comparison

3.2.1. Models of this study

To evaluate how the models perform on different species and on single- and multi-stemmed samples and species a comparison of CV and bias was made. Using the selected models in the categories *all models*, *main stem* and *basic models* for all samples, CV and bias of subsets of the data were calculated based on the estimate of the equations. The values of these general models are here compared to the CV and bias calculated on the estimate of the selected models specific for the subset in the same categories. Figures 2–4 (c) and (d) summaries the comparisons of selected models in the different categories, while (a) and (b) of the same figures visualize the estimated AGB from the equations in relation to the observed AGB.

The variance measurements are all higher in the general models than the species-specific models and increases with restrictions in variables selections (model categories) for both general and specific models, with few exceptions. Mean CV for different species in the general models are 0.49, 0.67 and 0.61 for categories *all models*, *main stem* and *basic models*, while median is 0.45, 0.56 and 0.61, respectively. The means of species-specific models are 0.13, 0.19 and 0.37, respectively. The larger mean of the general *main stem*-model is mainly caused by an increase of variance *B. micrantha* due to one largely overestimated sample. CV of the general model for the species is much larger (1.5) in this category than in *all models* and *basic models* (0.44 and 0.49, respectively). For *E. excelsum*, a decrease of CV for the general models is seen correlating with model simplicity as the CV for models in category *all models*, *main stem* and *basic models* are 0.30, 0.27 and 0.16, respectively. A notably large change in CV in both the general and the specific models is seen in *P. fulva*, with an increase in the general models from 0.50 in category *all models* to 0.98 and 1.04 in *main stem* and *basic models*, respectively, while the CV for species specific models increase with about 0.45 units for every category from 0.05 in *all models* to 0.97 *basic models*. An overall large CV for the general models is seen for *N. buchananii* increasing with restricting model variable selection (0.73, 0.69 and 0.84), while CV for the specific models remains low (0.10 and 0.11 for categories *all models* and *basic models*, respectively).

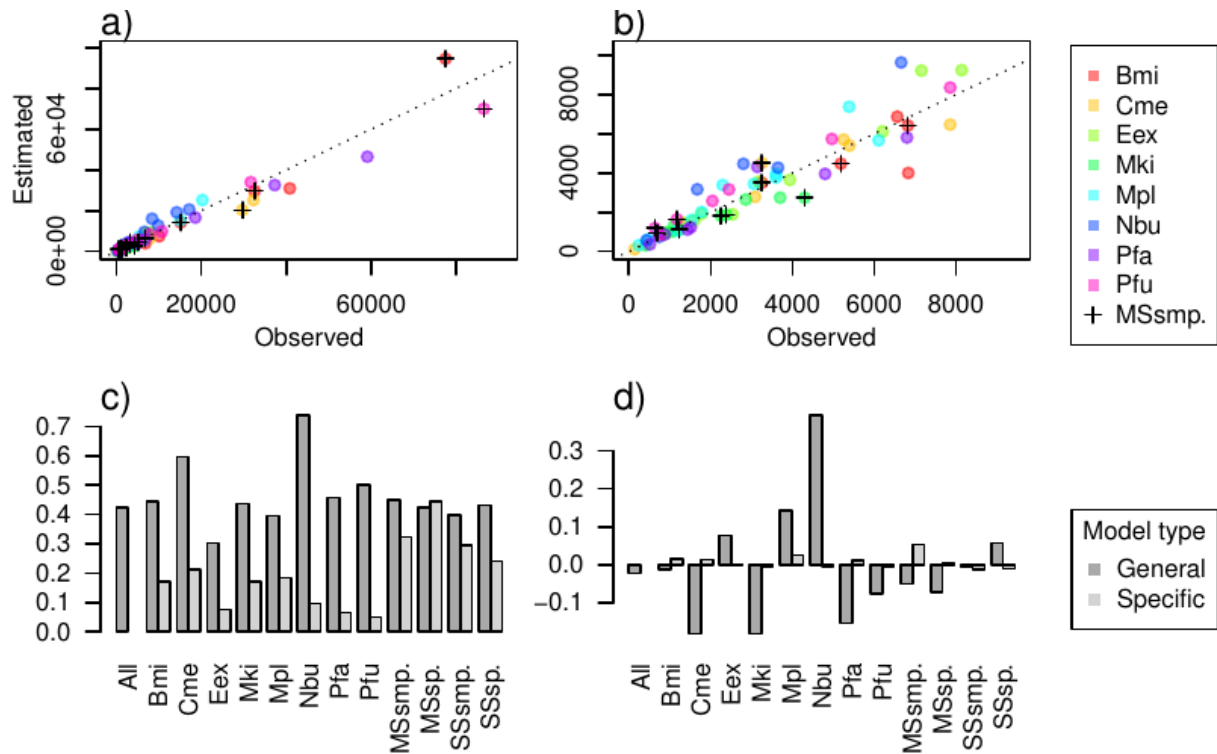


Figure 2. A summary of estimation of AGB of *Model.p.d².s_{sum}.NS* fitted on all samples. (a) plots estimated and observed AGB (g). (b) is an enlargement of the region closest to origo (10th percentile of the axes) of figure (a). Crosses indicate multi-stemmed samples and colors represent species: *B. micrantha* (Bmi), *C. megalocarpus* (Cme), *E. excelsum* (Eex), *M. kilimandscharica* (Mki), *M. platycalyx* (Mpl), *N. buchananii* (Nbu), *P. falcatus* (Pfa) and *P. fulva* (Pfu). The dotted line follows the slope of a 1:1-ratio. (c) and (d) show CV and bias, respectively, for the different subsets of the data. Dark grey bars are values based on estimates from mentioned model. Light grey bars are values based on the selected models for each subset in the category all models. MSsmp. and MSsp. are multi-stemmed samples and species, respectively; SSsmp. and SSsp. are single-stemmed samples and species, respectively.

The mean bias is close to 0 for species specific models, with a few notably large values. For *P. fulva* the selected model of category *main stem* yields an average underestimation of 5% biomass with an increased value for the basic model (11%). An on average 10% underestimation is also seen in the local model of *C. megalocarpus* and 5% for *M. kilimandscharica* in the category *basic models*. Larger bias is expected of the general model, with a mean of the different species bias of 15% for *all models*, 19% for category *main stem* and 22% for *basic models*. Most species remain under 20% bias for all categories. General models yield a large overestimation of biomass in *N. buchananii* with 40% and 38% for both selected model categories *all models* and *main stem*, respectively and 52% overestimation in the *basic model*. Most species are either overestimated or underestimated in all categories, with some notable exceptions. The general model of category *all models* exhibits low bias for *B. micrantha* while an overestimation of 22% is seen in the *main stem*-model. The bias shifts to and underestimation of 28% in the *basic model*. Also *P. falcatus* is overestimated (by 23%) in this category, while an underestimation is yielded for categories *all models* and *main stem* (15% and 13%, respectively).

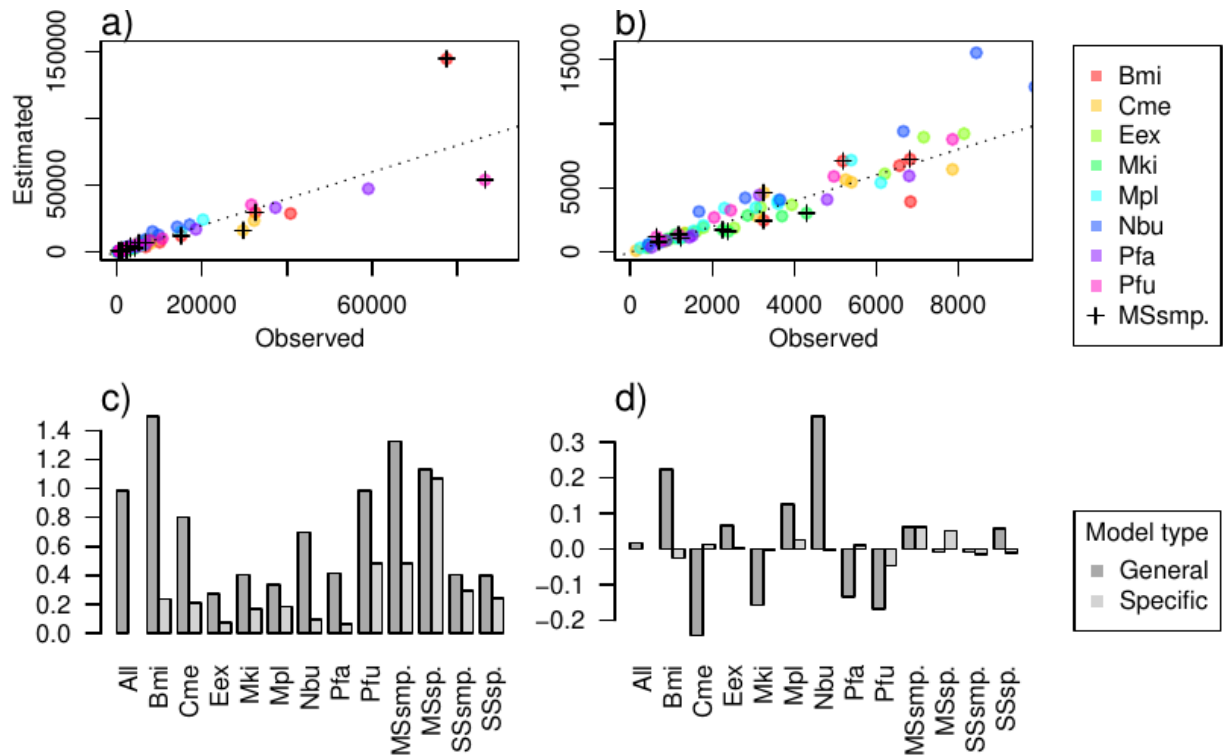


Figure 3. A summary of estimation of AGB of *Model.p.d².s.NS* fitted on all samples. (a) plots estimated and observed AGB (g). (b) is an enlargement of the region closest to origo (10th percentile of the axes) of figure (a). Crosses indicate multi-stemmed samples and colors represent species (see caption of figure 2 for species abbreviations). The dotted line follows the slope of a 1:1-ratio. (c) and (d) show CV and bias, respectively, for the different subsets of the data. Dark grey bars are values based on estimates from mentioned model. Light grey bars are values based on the selected models for each subset in the category main stem. MSsmp. and MSsp. are multi-stemmed samples and species, respectively; SSsmp. and SSsp. are single-stemmed samples and species, respectively.

The mean CV for models specific to single- or multi-stemmed samples or species are 0.32, 0.49 and 0.20 in order of increasing variable restrictions for the models. The calculated CV for these subsets when biomass was estimated by the general model yields a mean of 0.42 for the category *all models*, 0.82 for *main stem* and 0.64 for *basic models*, with a maximum of 1.33 for multi-stemmed samples and the second highest for multi-stemmed species (1.13), both in the second model category. The subset of multi-stemmed species also holds the highest CV for specific models at 1.1 (in the same category). Both multi-stemmed subsets exhibit the same pattern of having the highest CV in model category *main stem* in the general models as well as the specific. The lowest CV for multi-stemmed samples is found in the basic model specific for the subset (0.20), while the lowest for the multi-stemmed species is found in the overall best performing model fitted on all samples (0.42). The subsets of single-stemmed species and samples exhibits a more straight forward pattern of increasing CV when restricting model variables, regarding both general and specific models. Bias for multi-stemmed and single-stemmed subsets increases for the selected models for all samples, when restricting models to basic variables. The mean of the bias estimates of the general model is 5% and 3% for category *all models* and *main stem* but 25% for the basic model, with underestimations for multi-stemmed species and samples (20% and 35%, respectively) and overestimation of single-stemmed species and samples (26% and 17%, respectively). The general models have a notably low bias in categories *all models* and *main stem* for single-stemmed samples and in multi-stemmed species in category *Main stem* (below 1%). The local models of multi-stemmed subsets exhibit comparably high bias values with 4–6% overestimation in multi-stemmed samples (*all model* category) and in multi-stemmed species for the category *main stem*.

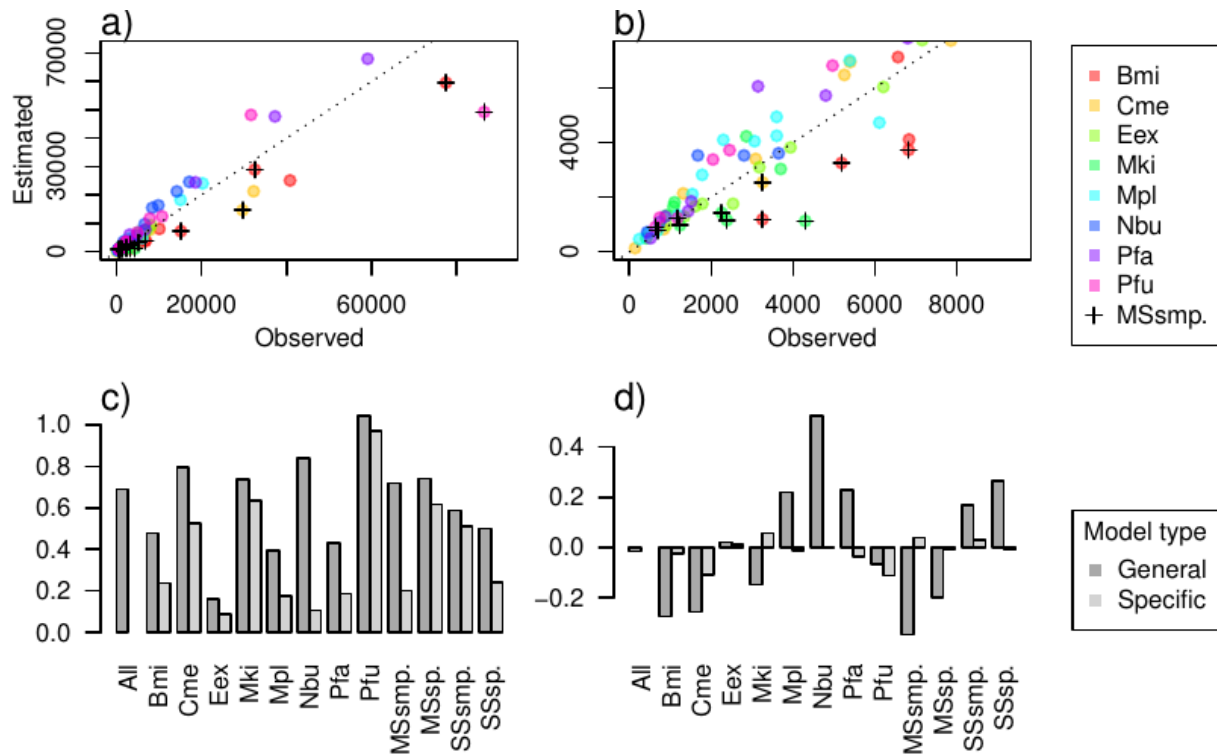


Figure 4. A summary of estimation of AGB of Model. $\rho.d^2$ fitted on all samples. (a) plots estimated and observed AGB (g). (b) is an enlargement of the region closest to origo (10th percentile of the axes) of figure (a). Crosses indicate multi-stemmed samples and colors represent species (see caption of figure 2 for species abbreviations). The dotted line follows the slope of a 1:1-ratio. (c) and (d) show CV and bias, respectively, for the different subsets of the data. Dark grey bars are values based on estimates from mentioned model. Light grey bars are values based on the selected models for each subset in the category basic models. MSsmp. and MSsp. are multi-stemmed samples and species, respectively; SSsmp. and SSsp. are single-stemmed samples and species, respectively.

3.2.2. Literature models

Among the equations from the literature Model 3 has the lowest variance of estimated AGB for all samples (Table 20). An overestimation of 4% is comparable with the 2% underestimation of the simplest model developed in this study and the CV is only slightly higher (0.73 compared to 0.68 for Model. $\rho.d^2$). Highest CV and bias were found in Model 1 with a CV of 1.02 and a bias of -29%. The adjusted Model 2 is intermediate in both variance and bias with a CV of 0.77 and an overestimation of 15% of mean AGB. Both models from Ali et al. (2015) show similar CV (0.98-1.01). Model 5 underestimates the AGB by 8%, while Model 4 yields the lowest bias of all literature models at -3%.

Table 20. A summary of CV and bias of AGB estimated for all samples from the equations found in literature. Model. $\rho.d^2$ from this study is added for comparison.

| | CV | Bias |
|-------------------|------|-------|
| Model 1 | 1.02 | -0.29 |
| Model 2 | 0.77 | 0.15 |
| Model 3 | 0.73 | 0.04 |
| Model 4 | 0.98 | -0.03 |
| Model 5 | 1.01 | -0.08 |
| Model. $\rho.d^2$ | 0.69 | -0.02 |

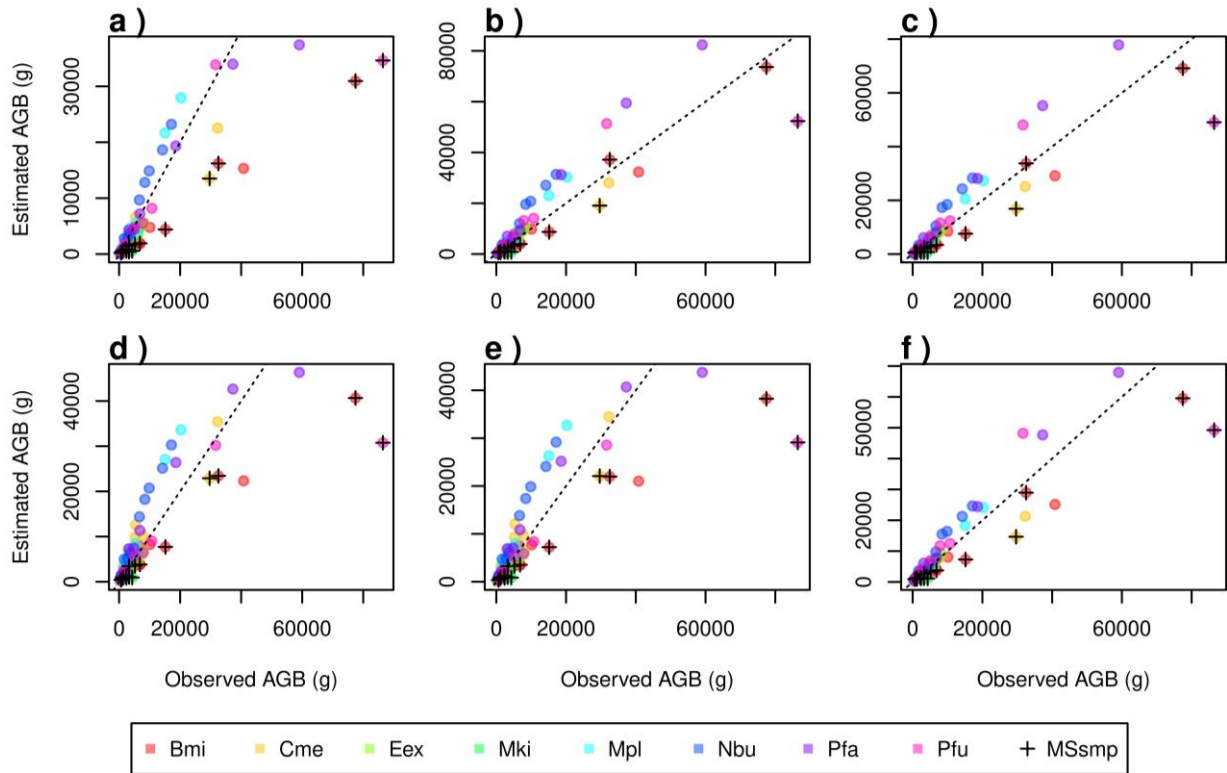


Figure 5. Plotting estimated AGB against observed AGB for different models. (a), (b) and (c) are Models 1-3 from Chave et al (2014 and 2005). (d) and (e) are Models 4-5 from Ali et al. (2015) and (f) is Model.p.d² from this study, for comparison. Crosses indicate multi-stemmed samples and colors represent species (see caption of figure 2 for species abbreviations). The dotted line follows the slope of a 1:1-ratio.

The overall accuracy of the estimates is well illustrated in Figure 5, where the difference in how subsets propagate in relation to the 1:1-ratio line is clear. To determine if and how the equations' estimates vary between subsets, the CV and bias of these estimates for different species, single- and multi-stemmed species and sample were compared (Figure 6 and 7).

All equations underestimate multi-stemmed samples and species similar to Model.p.d². The largest bias of multi-species subsets is found in Model 1 at -60% for multi-stemmed samples, but relatively small bias for single-stemmed samples (-12%) and very low for single-stemmed species (-1%) when grouped together. This also reflects in a large difference in CV between multi-stemmed groups (>1.1) and single-stemmed groups (<0.67). Similar difference, but higher CV, is yielded by Model 4 and 5. In comparison to Model 1, Models 2-5 show less bias for multi-stemmed groups but instead overestimates the single-stemmed species and samples, as do Model.p.d². The difference in bias between single- and multi-stemmed samples is slightly smaller in Model 1 than in Model.p.d², while Model 4 and 5 has the highest difference (bias_Δ range from 0.46 for Model 1 to 0.69 for Model 4). Opposite to Model 1, 4, 5 and Model.p.d², Models 2 and 3 have larger relative variance (CV) for single-stemmed subsets than multi-stemmed, but for Model 3 the difference is small. When accounting for the overall bias of the models the pattern over the different subsets (multi-species as well as for single species) is similar in all literature models as for Model.p.d². A large overestimation of *N. buchananii* is obvious in all the models. CV for this species is however lowest in Model 1 and small in comparison to several other species in this model. *P. fulva* is underestimated in Models 1 and more so in Model 4 and 5 but has a low bias in Models 2-3 and in Model.p.d² yet yields a large CV in these models as well.

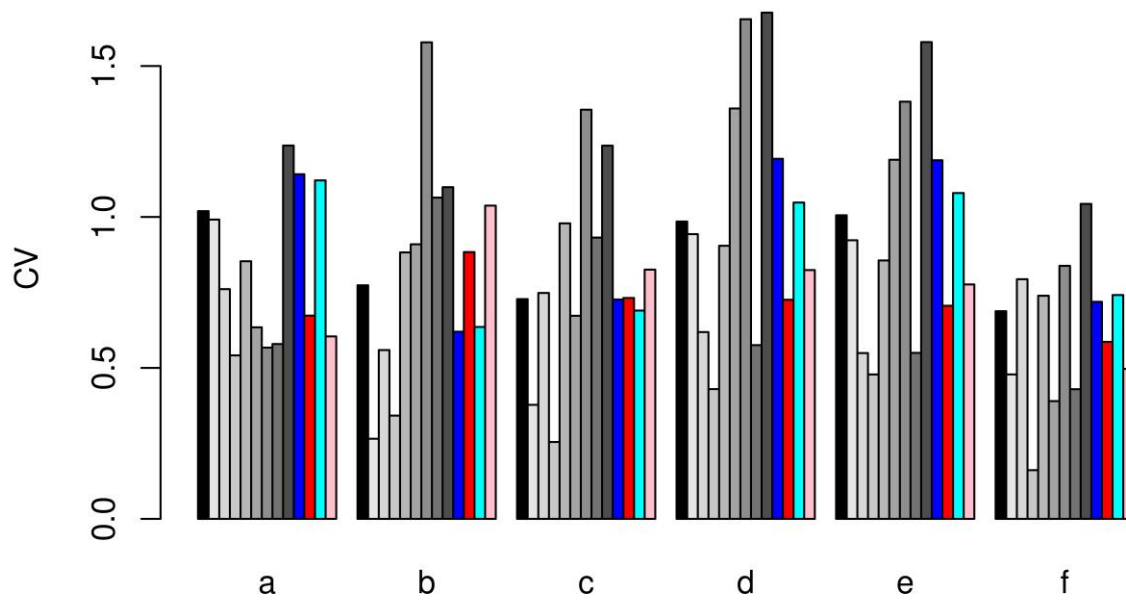


Figure 6. CV for different subsets based on the estimated AGB of equations from the literature. (a), (b) and (c) are Models 1-3 from Chave et al (2014, 2005). (d) and (e) are Models 4-5 from Ali et al. (2015) and (f) is Model $\rho.d^2$ from this study for comparison. Color of bars indicate different datasets: black bar is CV of all samples; grey gradient is species from the left: *B. micrantha*, *C. megalocarpus*, *E. excelsum*, *M. kilimandscharica*, *M. platycalyx*, *N. buchananii*, *P. falcatus* and *P. fulva*; blue and light blue are multi-stemmed samples and species, respectively; and red and pink bars are single-stemmed samples and species, respectively.

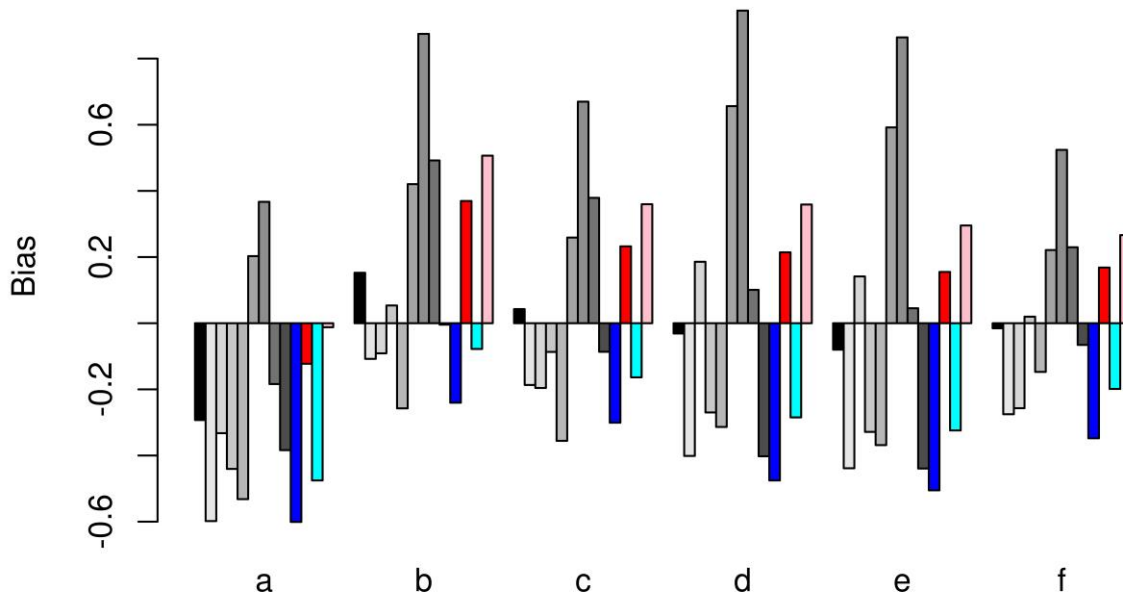


Figure 7. Bias for different subsets based on the estimated AGB of equations from the literature. (a), (b) and (c) are Models 1-3 from Chave et al (2014, 2005). (d) and (e) are Models 4-5 from Ali et al. (2015) and (f) is Model.p.d² from this study, for comparison. Color of bars indicate different datasets: black bar is CV of all samples; grey gradient is species from the left: *B. micrantha*, *C. megalocarpus*, *E. excelsum*, *M. kilimandscharica*, *M. platycalyx*, *N. buchananii*, *P. falcatus* and *P. fulva*; blue and light blue are multi-stemmed samples and species, respectively; and red and pink bars are single-stemmed samples and species, respectively.

4. Discussion

4.1. Models of this study

The predictor variables that best explained the variation of AGB in all samples were ρ , d^2 , s_{sum} and NS . ρ and d^2 alone explained 91% of the variation but generated an underestimation of multi-stemmed samples and an overestimation of single-stemmed samples. Addition of s_{sum} improved the accuracy and reduced the bias for variation in stem numbers. Stem count (NS) improved this model slightly while the model with s instead of s_{sum} showed a large improvement by NS . In fact, stem count together with ρ and d^2 explained slightly more of the variation than ρ , d^2 and s did (R^2 of 0.94 and 0.93 respectively). Using Model.p.d².s.NS would reduce labor demand when estimating AGB for multi-stemmed samples by limiting the number of precise diameter measurements. The preference for NS over s , leads to the conclusion that stem count would be the single most efficient way to increase accuracy (together with DBH and ρ). Using a prepared “fixed caliper” set at the lower limit for stem count inclusion makes this measurement fast and easy. As can be seen in Figure 2–3, the overall AGB estimate does not differ very much between Model.p.d².s.NS and Model.p.d².s_{sum}.NS, however the former largely overestimates one sample of *B. micrantha*, which represents a large tree with the highest number of stems among all samples. There is one notable difference between these two models regarding the sign of the coefficient of NS . While this coefficient in Model.p.d².s.NS is positive, compensating for the additional stemmed otherwise not accounted for in the model; the coefficient in Model.p.d².s_{sum}.NS is negative, compensation for the otherwise overestimation of many additional secondary stems. Both equations hold for most of the samples, but the former fails in this mentioned sample due to the large number of stems and the fact that most AGB is allocated to the main stem (68% of total AGB).

If there is a need for using a multi-species equation and to minimize labor, Model. $\rho.d^2$ would be biased for both single-stemmed and multi-stemmed samples. Two different equations for these subsets could instead be used, possibly with the added predictor variable h . For consistency the same model structure (Model. $\rho.d^2.h$) could be used. However, more sampling of multi-stemmed trees is needed to establish a stronger estimate of β_h .

As expected, wood density improves all multi-species models' performance with a highly significant coefficient with the exception of best performing model in the single-stemmed species subset. If applied to these species only, ρ could be excluded as a predictor variable but the low variation in this case might not be representative to a wider range of species hence, application onto other species could induce bias to the model. The d^2 is the overall most useful predictor variable in this study, as have been shown in many other studies. Polynomial of this measurement or the one-dimensional alone perform poorer for all models except for *C. megalocarpus*. The alternative measurement at 0.3 m above ground is in general more helpful as a complement to the breast height measurement. Differences in tapering could reveal architectural differences between the trees (e.g., branching or variation in diameter-to-height ratio). As exceptions to this, the single-species models of *M. platyalyx* and *P. falcatus* perform better with s or s^2 as the single diameter variable but the difference is small ($R^2_{\Delta} < 0.015$).

Height proves to not be of large importance in the majority of the models. The small improvement of R^2 of the basic model of all samples is bated by the non-significant difference between Model. $\rho.d^2.h$ and Model. $\rho.d^2$. As variation in the relationship between height and diameter has been shown to be lower between trees exposed to the same environmental factors and since most samples were collected at the two lower sites (with the exception of all *M. kilimandscharica* and 4 *M. platyalyx* samples), diameter could be enough to explain the allometric of the trees. The data collected in this study do however indicate a significant difference in height-to-diameter ratio between species (results not shown). Yet, models for several of the subsets perform better with height as a variable, especially when multiple diameters and CA is excluded. Interestingly, most species-specific models for the single-stemmed species in the category *basic models* perform best with height as a predictor variable, as do both the subsets of multi-stemmed and single-stemmed samples but not multi-stemmed and single-stemmed species. This could indicate that the height is not a good predictor of AGB when mixing single- and multi-stemmed samples.

CA is not included in most of the best performing models, when stem count and additional diameter measurements are available. When excluding these variables extension by CA improves the models to some extent (e.g., R^2 increase from 0.91 to 0.92 in Model. $\rho.d^2.CA$), but my experience is questioning this measurement's practical use for several reasons. Although it can be relatively easy and fast to measure it demands two persons in the procedure (stretching the measuring tape across the crown). Also, the determination of the angle to measure and how far the crown stretches is subjective to some degree, which could lead to inaccurate and biased measurements.

The overall lower CV for species-specific models and the over- and underestimation of different species in the general models, show the superiority of species-specific equations of accurate AGB estimates. Some species have a particularly large bias in all general models (e.g., *N. buchananii* ranging from 38% to 52%). Since most of the variation between species in the general model correlates with the bias of the species, including taxonomy in the models could largely improve them. In some cases, even the species-specific model fails in explaining a large portion of the variation in AGB. *C. megalocarpus*, *M. kilimandscharica* and *P. fulva*, in particular yielded large CV in the *basic models* category (0.97 for *P. fulva*) and with a notably low R^2 at 0.34 for *M. kilimandscharica*. These three species all have few multi-stemmed samples (2, 4 and 3 out of 10, respectively). In contrast 6 out of 10 of the samples of *B. micrantha* are multi-stemmed, which could help to lower the CV of the specific model in comparison to the general.

The large CV for the subset of multi-stemmed species in both the general and the specific models in the category *basic models* and the large difference between the general and the specific models

for multi-stemmed samples, indicates a difference in allometry for single- and multi-stemmed tree that is not accounted for with the basic variables. Due to the restriction in sampling only a small sample size of multi-stemmed trees was obtained in relation to single-stemmed, which reflects in the higher bias for multi-stemmed samples in general models. If one aims to estimate AGB equally accurately for trees in both these two categories more effort is needed to sample more multi-stemmed samples.

4.2. Models from literature

Regarding the validity of the models found in the literature, Model 3 (Chave et al., 2005) gives a good estimate of the total AGB of the samples with a bias of only 4%. The CV of this model is very similar to the CV of the basic model developed for these particular samples. The model is clearly biased regarding both species and single- and multi-stemmed species, but again not to a larger degree than the model developed in this study. The combination of the second and third dimension of d seems to compensate for the overestimation of single-stemmed samples to some degree, without increasing the underestimation of multi-stemmed samples to the same extent. The adjustment of Model 2 (modified from Chave et al., 2014) fails in obtaining an unbiased estimate, due to the heteroscedasticity of the data in the untransformed scale. The discrepancy between Model 1 and 2 (see Figure 5) indicates that the relationship of height and diameter is not the same in these samples as in the equation used to estimate height from diameter in the transformation of Model 1 into Model 2. Interestingly, most of the single-stemmed but not multi-stemmed samples are well estimated in Model 1, further arguing for the variation of allometry between these two groups. Model 4 yields the lowest bias on the total AGB but also a large CV and variation of bias between different subsets, similar to Models 1 and 5. The inclusion of height in these models could explain the discrepancy. As found by Ali et al. (2015), CA is not improving models much when applied to different species.

The distribution of trees along the size range regarding height (and diameter) was fairly even but due to the nature of the relationship of these dimensions to AGB, the result of the sample selection led to a few samples with much larger AGB than the median. These samples have an unproportional influence on CV and bias calculations. This is suitable when a stand estimate is of interest, but these parameters lack information of how well the equations estimate AGB in relation to the tree size. If, for example, relative growth rate for individual trees is of interest, a measurement of variance and bias relative to the individual tree might be more suitable.

To properly test the validity of the equations developed in this study and to compare them to the performance of other equations, new data must be collected and compared with the equations estimates. Especially if one aims to estimate AGB for other species or at other sites.

4.3. Conclusion

To conclude, the study shows that the equation from Chave et al. (2005) for moist forest without height performs best of the available equations tested. It overestimated total AGB by 4%. The variance was 73% of mean AGB for individual tree estimates, only slightly larger than the simplest model developed here, based on the samples. The combination of ρ , DBH, sum of diameter at 0.3 m and a stem count performed best on the pooled data. Species-specific equations decreased variance to below 20% in most cases, for the simplest models and is recommended. Regarding additional predictor variables (besides ρ , DBH and height) the sum of the diameters at 0.3 m explained most of variance in the datasets with multi-stemmed samples included. The most practically efficient measurement to add would be a stem count at 0.3 m above ground.

References

Abich, A., Negash, M., Alemu, A., & Gashaw, T. (2022). Aboveground Biomass Models in the Combretum-Terminalia Woodlands of Ethiopia: Testing Species and Site Variation Effects. *Land (Basel)*, 11(6), 811. <https://doi.org/10.3390/land11060811>

- Ali, A., Xu, M.-S., Zhao, Y.-T., Zhang, Q.-Q., Zhou, L.-L., Yang, X.-D., & Yan, E.-R. (2015). Allometric biomass equations for shrub and small tree species in subtropical China. *Silva Fennica (Helsinki, Finland : 1967)*, 49(4). <https://doi.org/10.14214/sf.1275>
- Anderson-Teixeira, K. J., McGarvey, J. C., Muller-Landau, H. C., Park, J. Y., Gonzalez-Akre, E. B., Herrmann, V., Bennett, A. C., So, C. V., Bourg, N. A., Thompson, J. R., McMahon, S. M., McShea, W. J., Sayer, E., & Sayer, E. (2015). Size-related scaling of tree form and function in a mixed-age forest. *Functional Ecology*, 29(12), 1587–1602. <https://doi.org/10.1111/1365-2435.12470>
- Asuero, A. G., & Bueno, J. M. (2011). Fitting Straight Lines with Replicated Observations by Linear Regression. IV. Transforming Data. *Critical Reviews in Analytical Chemistry*, 41(1), 36–69. <https://doi.org/10.1080/10408347.2010.523589>
- Baker, T. R., Phillips, O. L., Malhi, Y., Almeida, S., Arroyo, L., Di Fiore, A., Erwin, T., Killeen, T. J., Laurance, S. G., & Laurance, W. F. (2004). Variation in wood density determines spatial patterns in Amazonian forest biomass. *Global Change Biology*, 10(5), 545–562. <https://doi.org/10.1111/j.1365-2486.2004.00751.x>
- Banin, L., Feldpausch, T. R., Phillips, O. L., Baker, T. R., Lloyd, J., Affum-Baffoe, K., Arets, E. J. M. M., Berry, N. J., Bradford, M., Brienen, R. J. W., Davies, S., Drescher, M., Higuchi, N., Hilbert, D. W., Hladik, A., Iida, Y., Salim, K. A., Kassim, A. R., King, D. A., ... Lewis, S. L. (2012). What controls tropical forest architecture? Testing environmental, structural and floristic drivers. *Global Ecology and Biogeography*, 21(12), 1179–1190. <https://doi.org/10.1111/j.1466-8238.2012.00778.x>
- Baskerville, G. L. (1972). Use of logarithmic regression in the estimation of plant biomass. *Canadian Journal of Forest Research*, 2(1), 49-53.
- Burrows, W. H., Hoffmann, M. B., Compton, J. F., Back, P. V., & Tait, L. J. (2000). Allometric relationships and community biomass estimates for some dominant eucalypts in Central Queensland woodlands. *Australian Journal of Botany*, 48(6), 707-714.
- Brienen, R. J. W., Phillips, O. L., Feldpausch, T. R., Gloor, E., Baker, T. R., Lloyd, J., Lopez-Gonzalez, G., Monteagudo-Mendoza, A., Malhi, Y., Lewis, S. L., Vasquez Martinez, R., Alexiades, M., Alvarez Davila, E., Alvarez-Loayza, P., Andrade, A., Aragao, L. E. O. C., Araujo-Murakami, A., Arets, E. J. M. M., Arroyo, L., ... Zagt, R. J. (2015). Long-term decline of the Amazon carbon sink. *Nature (London)*, 519(7543), 344–348. <https://doi.org/10.1038/nature14283>
- Brown, S., & Lugo, A. E. (1984). Biomass of tropical forests: a new estimate based on forest volumes. *Science (American Association for the Advancement of Science)*, 223(4642), 1290–1293. <https://doi.org/10.1126/science.223.4642.1290>
- Brown, S., Gillespie, A. J., & Lugo, A. E. (1989). Biomass estimation methods for tropical forests with applications to forest inventory data. *Forest science*, 35(4), 881-902.
- Brown, I. F., Martinelli, L. A., Thomas, W. W., Moreira, M. Z., Cid Ferreira, C. A., & Victoria, R. A. (1995). Uncertainty in the biomass of Amazonian forests: An example from Rondônia, Brazil. *Forest Ecology and Management*, 75(1), 175–189. [https://doi.org/10.1016/0378-1127\(94\)03512-U](https://doi.org/10.1016/0378-1127(94)03512-U)
- Chambers, J. Q., Santos, J. dos, Ribeiro, R. J., & Higuchi, N. (2001). Tree damage, allometric relationships, and above-ground net primary production in central Amazon forest. *Forest Ecology and Management*, 152(1), 73–84. [https://doi.org/10.1016/S0378-1127\(00\)00591-0](https://doi.org/10.1016/S0378-1127(00)00591-0)

- Chave, J., Riéra, B., & Dubois, M.-A. (2001). Estimation of biomass in a neotropical forest of French Guiana: spatial and temporal variability. *Journal of Tropical Ecology*, *17*(1), 79–96. <https://doi.org/10.1017/S0266467401001055>
- Chave, J., Condit, R., Lao, S., Caspersen, J. P., Foster, R. B., & Hubbell, S. P. (2003). Spatial and Temporal Variation of Biomass in a Tropical Forest: Results from a Large Census Plot in Panama. *The Journal of Ecology*, *91*(2), 240–252. <https://doi.org/10.1046/j.1365-2745.2003.00757.x>
- Chave, J., Condit, R., Aguilar, S., Hernandez, A., Lao, S., Perez, R., Phillips, O. L., & Malhi, Y. (2004). Error propagation and scaling for tropical forest biomass estimates. *Philosophical Transactions of the Royal Society of London. Series B. Biological Sciences*, *359*(1443), 409–420. <https://doi.org/10.1098/rstb.2003.1425>
- Chave, J., Andalo, C., Brown, S., Cairns, M. A., Chambers, J. Q., Eamus, D., Folster, H., Fromard, F., Higuchi, N., & Kira, T. (2005). Tree allometry and improved estimation of carbon stocks and balance in tropical forests. *Oecologia*, *145*(1), 87–99. <https://doi.org/10.1007/s00442-005-0100-x>
- Chave, J., Réjou-Méchain, M., Búrquez, A., Chidumayo, E., Colgan, M. S., Delitti, W. B. C., Duque, A., Eid, T., Fearnside, P. M., Goodman, R. C., Henry, M., Martínez-Yrizar, A., Mugasha, W. A., Muller-Landau, H. C., Mencuccini, M., Nelson, B. W., Ngomanda, A., Nogueira, E. M., Ortiz-Malavassi, E., ... Vieilledent, G. (2014). Improved allometric models to estimate the aboveground biomass of tropical trees. *Global Change Biology*, *20*(10), 3177–3190. <https://doi.org/10.1111/gcb.12629>
- Chenge, I. B. (2021). Height–diameter relationship of trees in Omo strict nature forest reserve, Nigeria. *Trees, Forests and People (Online)*, *3*, 100051. <https://doi.org/10.1016/j.tfp.2020.100051>
- Clark, D. B., & Clark, D. A. (2000). Landscape-scale variation in forest structure and biomass in a tropical rain forest. *Forest Ecology and Management*, *137*(1), 185–198. [https://doi.org/10.1016/S0378-1127\(99\)00327-8](https://doi.org/10.1016/S0378-1127(99)00327-8)
- Clark, D. A., Brown, S., Kicklighter, D. W., Chambers, J. Q., Thomlinson, J. R., & Ni, J. (2001). Measuring Net Primary Production in Forests: Concepts and Field Methods. *Ecological Applications*, *11*(2), 356–370. [https://doi.org/10.1890/1051-0761\(2001\)011\[0356:MNPPIF\]2.0.CO;2](https://doi.org/10.1890/1051-0761(2001)011[0356:MNPPIF]2.0.CO;2)
- Clark, D. A., Phillips, O. L., Malhi, Y., Phillips, O. L., & Malhi, Y. (2004). Sources or sinks? The responses of tropical forests to current and future climate and atmospheric composition. *Philosophical Transactions of the Royal Society of London. Series B. Biological Sciences*, *359*(1443), 477–491. <https://doi.org/10.1098/rstb.2003.1426>
- Clifford, D., Cressie, N., England, J. R., Roxburgh, S. H., & Paul, K. I. (2013). Correction factors for unbiased, efficient estimation and prediction of biomass from log–log allometric models. *Forest Ecology and Management*, *310*, 375–381. <https://doi.org/10.1016/j.foreco.2013.08.041>
- Cole, T. G., & Ewel, J. J. (2006). Allometric equations for four valuable tropical tree species. *Forest Ecology and Management*, *229*(1), 351–360. <https://doi.org/10.1016/j.foreco.2006.04.017>
- Conti, G., Enrico, L., Casanoves, F., & Díaz, S. (2013). Shrub biomass estimation in the semiarid Chaco forest: a contribution to the quantification of an underrated carbon stock. *Annals of Forest Science.*, *70*(5), 515–524. <https://doi.org/10.1007/s13595-013-0285-9>
- da Costa, A. C. L., Galbraith, D., Almeida, S., Takeshi, B., Portela, T., da Costa, M., de Athaydes Silva Junior, J., Braga, A. P., de Gonçalves, P. H. L., de Oliveira, A. A., Fisher, R., Phillips, O. L., Metcalfe, D. B., Levy, P., & Meir, P. (2010). Effect of 7 yr of experimental drought on vegetation

dynamics and biomass storage of an eastern Amazonian rainforest. *The New Phytologist*, 187(3), 579–591. <https://doi.org/10.1111/j.1469-8137.2010.03309.x>

Deans, J. D., Moran, J., & Grace, J. (1996). Biomass relationships for tree species in regenerating semi-deciduous tropical moist forest in Cameroon. *Forest Ecology and Management*, 88(3), 215–225. [https://doi.org/10.1016/S0378-1127\(96\)03843-1](https://doi.org/10.1016/S0378-1127(96)03843-1)

DeWalt, S. J., & Chave, J. (2004). Structure and biomass of four lowland neotropical forests. *Biotropica*, 36(1), 7–19. <https://doi.org/10.1111/j.1744-7429.2004.tb00291.x>

Doughty, C. E., Keany, J. M., Wiebe, B. C., Rey-Sanchez, C., Carter, K. R., Middleby, K. B., Cheesman, A. W., Goulden, M. L., da Rocha, H. R., Miller, S. D., Malhi, Y., Fauset, S., Gloor, E., Slot, M., Oliveras Menor, I., Crous, K. Y., Goldsmith, G. R., & Fisher, J. B. (2023). Tropical forests are approaching critical temperature thresholds. *Nature (London)*, 621(7977), 105–111. <https://doi.org/10.1038/s41586-023-06391-z>

Enquist, B. J., Brown, J. H., & West, G. B. (1998). Allometric scaling of plant energetics and population density. *Nature (London)*, 395(6698), 163–165. <https://doi.org/10.1038/25977>

Fayolle, A., Doucet, J.-L., Gillet, J.-F., Bourland, N., & Lejeune, P. (2013). Tree allometry in Central Africa: Testing the validity of pantropical multi-species allometric equations for estimating biomass and carbon stocks. *Forest Ecology and Management*, 305, 29–37. <https://doi.org/10.1016/j.foreco.2013.05.036>

Fearnside, P. M. (1997). Wood density for estimating forest biomass in Brazilian Amazonia. *Forest Ecology and Management*, 90(1), 59–87. [https://doi.org/10.1016/S0378-1127\(96\)03840-6](https://doi.org/10.1016/S0378-1127(96)03840-6)

Feldpausch, T. R., Banin, L., Phillips, O. L., Baker, T. R., Lewis, S. L., Quesada, C. A., Affum-Baffoe, K., Arets, E. J. M. M., Berry, N. J., Bird, M., Brondizio, E. S., Camargo, P. de, Chave, J., Djangbletey, G., Domingues, T. F., Drescher, M., Fearnside, P. M., Franca, M. B., Fyllas, N. M., ... Lloyd, J. (2011). Height-diameter allometry of tropical forest trees. *Biogeosciences*, 8(5), 1081–1106. <https://doi.org/10.5194/bg-8-1081-2011>

Friedlingstein, P., O’Sullivan, M., Jones, M. W., Andrew, R. M., Hauck, J., Olsen, A., Peters, G. P., Peters, W., Pongratz, J., Sitch, S., Le Quéré, C., Canadell, J. G., Ciais, P., Jackson, R. B., Alin, S., Aragão, L. E. O. C., Arneeth, A., Arora, V., Bates, N. R., ... Zaehle, S. (2020). Global Carbon Budget 2020. *Earth System Science Data*, 12(4), 3269–3340. <https://doi.org/10.5194/essd-12-3269-2020>

Forster, M., & Sober, E. (1994). How to Tell When Simpler, More Unified, or Less Ad Hoc Theories will Provide More Accurate Predictions. *The British Journal for the Philosophy of Science*, 45(1), 1–35. <https://doi.org/10.1093/bjps/45.1.1>

Girardin, C. A. J., Malhi, Y., Aragão, L. E. O. C., Mamani, M., Huaraca Huasco, W., Durand, L., Feeley, K. J., Rapp, J., Silva-Espejo, J. E., Silman, M., Salinas, N., & Whittaker, R. J. (2010). Net primary productivity allocation and cycling of carbon along a tropical forest elevational transect in the Peruvian Andes. *Global Change Biology*, 16(12), 3176–3192. <https://doi.org/10.1111/j.1365-2486.2010.02235.x>

Goodman, R. C., Phillips, O. L., & Baker, T. R. (2014). The importance of crown dimensions to improve tropical tree biomass estimates. *Ecological Applications*, 24(4), 680–698. <https://doi.org/10.1890/13-0070.1>

Hunter, M. O., Keller, M., Victoria, D., & Morton, D. C. (2013). Tree height and tropical forest biomass estimation. *Biogeosciences*, 10(12), 8385–8399. <https://doi.org/10.5194/bg-10-8385-2013>

- Huxley, J.S. (1932) Problems of relative growth. Methuen, London. <https://dn790006.ca.archive.org/0/items/problemsofrelati00huxl/problemsofrelati00huxl.pdf>. Accessed 19 Dec, 2024.
- Kearsley, E., Moonen, P. C., Hufkens, K., Doetterl, S., Lisingo, J., Boyemba Bosela, F., Boeckx, P., Beekman, H., & Verbeeck, H. (2017). Model performance of tree height-diameter relationships in the central Congo Basin. *Annals of Forest Science.*, 74(1), 1–13. <https://doi.org/10.1007/s13595-016-0611-0>
- Ketterings, Q. M., Coe, R., van Noordwijk, M., Ambagau', Y., & Palm, C. A. (2001). Reducing uncertainty in the use of allometric biomass equations for predicting above-ground tree biomass in mixed secondary forests. *Forest Ecology and Management*, 146(1), 199–209. [https://doi.org/10.1016/S0378-1127\(00\)00460-6](https://doi.org/10.1016/S0378-1127(00)00460-6)
- King, D. A. (1986). Tree form, height growth, and susceptibility to wind damage in *Acer saccharum*. *Ecology (Durham)*, 67(4), 980–990. <https://doi.org/10.2307/1939821>
- King, D. A. (1996). Allometry and life history of tropical trees. *Journal of Tropical Ecology*, 12(1), 25–44. <https://doi.org/10.1017/S0266467400009299>
- King, D. A., Davies, S. J., M. N. Nur Supardi, & Tan, S. (2005). Tree Growth Is Related to Light Interception and Wood Density in Two Mixed Dipterocarp Forests of Malaysia. *Functional Ecology*, 19(3), 445–453. <https://doi.org/10.1111/j.1365-2435.2005.00982.x>
- Lewis, S., Lopez-Gonzalez, G., Sonké, B., Affum-Baffoe, K., Ojo, L., White, L., Hart, T., Hladik, A., Sheil, D., Swaine, M., Taylor, D., & Phillips, O. (2009). Increasing carbon storage in intact African tropical forests: Implications for the global carbon cycle. *IOP Conference Series. Earth and Environmental Science*, 6(8), 082009–1. <https://doi.org/10.1088/1755-1307/6/8/082009>
- Lima, A. J. N., Suwa, R., de Mello Ribeiro, G. H. P., Kajimoto, T., dos Santos, J., da Silva, R. P., de Souza, C. A. S., de Barros, P. C., Noguchi, H., Ishizuka, M., & Higuchi, N. (2012). Allometric models for estimating above- and below-ground biomass in Amazonian forests at São Gabriel da Cachoeira in the upper Rio Negro, Brazil. *Forest Ecology and Management*, 277, 163–172. <https://doi.org/10.1016/j.foreco.2012.04.028>
- Litton, C. M., & Boone Kauffman, J. (2008). Allometric Models for Predicting Aboveground Biomass in Two Widespread Woody Plants in Hawaii. *Biotropica*, 40(3), 313–320. <https://doi.org/10.1111/j.1744-7429.2007.00383.x>
- Magarik, Y. A. S., Roman, L. A., & Henning, J. G. (2020). How should we measure the DBH of multi-stemmed urban trees? *Urban Forestry & Urban Greening*, 47, 126481. <https://doi.org/10.1016/j.ufug.2019.126481>
- Malhi, Y., Doughty, C., & Galbraith, D. (2011). The allocation of ecosystem net primary productivity in tropical forests. *Philosophical Transactions of the Royal Society of London. Series B. Biological Sciences*, 366(1582), 3225–3245. <https://doi.org/10.1098/rstb.2011.0062>
- Marshall, A. R., Willcock, S., Platts, P. J., Lovett, J. C., Balmford, A., Burgess, N. D., Latham, J. E., Munishi, P. K. T., Salter, R., Shirima, D. D., & Lewis, S. L. (2012). Measuring and modelling above-ground carbon and tree allometry along a tropical elevation gradient. *Biological Conservation*, 154, 20–33. <https://doi.org/10.1016/j.biocon.2012.03.017>
- Mascaro, J., Litton, C. M., Hughes, R. F., Uowolo, A., & Schnitzer, S. A. (2011). Minimizing Bias in Biomass Allometry: Model Selection and Log-Transformation of Data. *Biotropica*, 43(6), 649–653. <https://doi.org/10.1111/j.1744-7429.2011.00798.x>

- Mascaro, J., & Schnitzer, S. A. (2011). Dominance by the introduced tree *Rhamnus cathartica* (common buckthorn) may limit aboveground carbon storage in Southern Wisconsin forests. *Forest Ecology and Management*, 261(3), 545–550. <https://doi.org/10.1016/j.foreco.2010.11.005>
- Mcculloh, K. A., Johnson, D. M., Meinzer, F. C., Voelker, S. L., Lachenbruch, B., & Domec, J.-C. (2012). Hydraulic architecture of two species differing in wood density: opposing strategies in co-occurring tropical pioneer trees. *Plant, Cell and Environment*, 35(1), 116–125. <https://doi.org/10.1111/j.1365-3040.2011.02421.x>
- Memiaghe, H. R., Lutz, J. A., Korte, L., Alonso, A., Kenfack, D., & Zang, R. (2016). Ecological Importance of Small-Diameter Trees to the Structure, Diversity and Biomass of a Tropical Evergreen Forest at Rabi, Gabon. *PloS One*, 11(5), e0154988–e0154988. <https://doi.org/10.1371/journal.pone.0154988>
- Miller, D. M. (1984). Reducing Transformation Bias in Curve Fitting. *The American Statistician*, 38(2), 124–126. <https://doi.org/10.1080/00031305.1984.10483180>
- Mitchard, E. T. A. (2018). The tropical forest carbon cycle and climate change. *Nature (London)*, 559(7715), 527–534. <https://doi.org/10.1038/s41586-018-0300-2>
- Montagu, K. D., Düttmer, K., Barton, C. V. M., & Cowie, A. L. (2005). Developing general allometric relationships for regional estimates of carbon sequestration—an example using *Eucalyptus pilularis* from seven contrasting sites. *Forest Ecology and Management*, 204(1), 115–129. <https://doi.org/10.1016/j.foreco.2004.09.003>
- Mugasha, W. A., Bollandsås, O. M., & Eid, T. (2013). Relationships between diameter and height of trees in natural tropical forest in Tanzania. *Southern Forests*, 75(4), 221–237. <https://doi.org/10.2989/20702620.2013.824672>
- Murphy, P. G., & Lugo, A. E. (1986). Structure and biomass of a subtropical dry forest in Puerto Rico. *Biotropica*, 18(2), 89–96. <https://doi.org/10.2307/2388750>
- Nogueira, E. M., Nelson, B. W., Fearnside, P. M., França, M. B., & Oliveira, Á. C. A. de. (2008a). Tree height in Brazil's 'arc of deforestation': Shorter trees in south and southwest Amazonia imply lower biomass. *Forest Ecology and Management*, 255(7), 2963–2972. <https://doi.org/10.1016/j.foreco.2008.02.002>
- Nogueira, E. M., Fearnside, P. M., Nelson, B. W., Barbosa, R. I., & Keizer, E. W. H. (2008b). Estimates of forest biomass in the Brazilian Amazon: New allometric equations and adjustments to biomass from wood-volume inventories. *Forest Ecology and Management*, 256(11), 1853–1867. <https://doi.org/10.1016/j.foreco.2008.07.022>
- Ntirugulirwa, B., Zibera, E., Epaphrodite, N., Manishimwe, A., Nsabimana, D., Uddling, J., & Wallin, G. (2023). Thermophilisation of Afromontane forest stands demonstrated in an elevation gradient experiment. *Biogeosciences*, 20(24), 5125–5149. <https://doi.org/10.5194/bg-20-5125-2023>
- Overman, J. P. M., Witte, H. J. L., & Saldarriaga, J. G. (1994). Evaluation of regression models for above-ground biomass determination in Amazon rainforest. *Journal of Tropical Ecology*, 10(2), 207–218. <https://doi.org/10.1017/S0266467400007859>
- Pan, Y., Birdsey, R. A., Phillips, O. L., Houghton, R. A., Fang, J., Kauppi, P. E., Keith, H., Kurz, W. A., Ito, A., Lewis, S. L., Nabuurs, G.-J., Shvidenko, A., Hashimoto, S., Lerink, B., Schepaschenko, D., Castanho, A., & Murdiyarso, D. (2024). The enduring world forest carbon sink. *Nature (London)*, 631(8021), 563–569. <https://doi.org/10.1038/s41586-024-07602-x>

- Pek, J., Wong, O., & Wong, A. C. (2017). Data Transformations for Inference with Linear Regression: Clarifications and Recommendations. *Practical Assessment, Research & Evaluation*, 22(9), 9. <https://doi.org/10.7275/2w3n-0f07>
- Picard, N., Saint-André, L., & Henry, M. (2012). Manual for building tree volume and biomass allometric equations: from field measurement to prediction. FAO; Food and Agricultural Organization of the United Nations.
- Poorter, L., Bongers, L., & Bongers, F. (2006). Architecture of 54 moist-forest tree species: traits, trade-offs, and functional groups. *Ecology (Durham)*, 87(5), 1289–1301. [https://doi.org/10.1890/0012-9658\(2006\)87\[1289:AOMTST\]2.0.CO;2](https://doi.org/10.1890/0012-9658(2006)87[1289:AOMTST]2.0.CO;2)
- Poorter, L., McDonald, I., Alarcón, A., Fichtler, E., Licona, J.-C., Peña-Claros, M., Sterck, F., Villegas, Z., & Sass-Klaassen, U. (2010). Importance of wood traits and hydraulic conductance for the performance and life history strategies of 42 rainforest tree species. *The New Phytologist*, 185(2), 481–492. <https://doi.org/10.1111/j.1469-8137.2009.03092.x>
- Rappaport, D. I., Morton, D. C., Longo, M., Keller, M., Dubayah, R., & dos-Santos, M. N. (2018). Quantifying long-term changes in carbon stocks and forest structure from Amazon forest degradation. *Environmental Research Letters*, 13(6), 65013. <https://doi.org/10.1088/1748-9326/aac331>
- Rozendaal, D. M. A., During, H. J., Sterck, F. J., Asscheman, D., Wiegerraad, J., & Zuidema, P. A. (2015). Long-term growth patterns of juvenile trees from a Bolivian tropical moist forest: shifting investments in diameter growth and height growth. *Journal of Tropical Ecology*, 31(6), 519–529. <https://doi.org/10.1017/S0266467415000401>
- Scaranello, M. A. da S., Alves, L. F., Vieira, S. A., Camargo, P. B. de, Joly, C. A., & Martinelli, L. A. (2012). Height-diameter relationships of tropical Atlantic moist forest trees in southeastern Brazil. *Scientia Agricola*, 69(1), 26–37. <https://doi.org/10.1590/S0103-90162012000100005>
- Shenkin, A., Bentley, L. P., Oliveras, I., Salinas, N., Adu-Bredu, S., Marimon-Junior, B. H., Marimon, B. S., Peprah, T., Choque, E. L., Trujillo Rodriguez, L., Clemente Arenas, E. R., Adonteng, C., Seidu, J., Passos, F. B., Reis, S. M., Blonder, B., Silman, M., Enquist, B. J., Asner, G. P., & Malhi, Y. (2020). The Influence of Ecosystem and Phylogeny on Tropical Tree Crown Size and Shape. *Frontiers in Forests and Global Change*, 3. <https://doi.org/10.3389/ffgc.2020.501757>
- Ter-Mikaelian, M. T., & Korzukhin, M. D. (1997). Biomass equations for sixty-five North American tree species. *Forest Ecology and Management*, 97(1), 1–24. [https://doi.org/10.1016/S0378-1127\(97\)00019-4](https://doi.org/10.1016/S0378-1127(97)00019-4)
- Thomas, S. C., Martin, A. R., Mycroft, E. E., & Bellingham, P. (2015). Tropical trees in a wind-exposed island ecosystem: height-diameter allometry and size at onset of maturity. *The Journal of Ecology*, 103(3), 594–605. <https://doi.org/10.1111/1365-2745.12378>
- West, G. B., Enquist, B. J., & Brown, J. H. (2009). general quantitative theory of forest structure and dynamics. *Proceedings of the National Academy of Sciences - PNAS*, 106(17), 7040–7045. <https://doi.org/10.1073/pnas.0812294106>

Appendix

Popular science summary

Human emission of carbon dioxide affects the climate and will change living conditions for humans as well as other organisms, all over the world. Plants use carbon dioxide from the atmosphere to produce biomass through photosynthesis. About 25% of the carbon released by human activity is taken up and stored by forest, the bulk of it in the tropics. To better understand how much carbon the tropical forests can store and how this will be affected by changes in climate and human land-use in the future, we need to improve our estimates of biomass in these ecosystems. This study is contributing to this by modeling the biomass of some tree species in the rainforest of Rwanda.

Allometry is the term describing the relationship of an organism's size and other measurements. For trees measurements of stem diameter, wood density and height are often used to estimate their biomass. However, a single model cannot accurately estimate the biomass of all trees. The architecture of trees varies between species but also depending on where they grow and their size. In a species-rich areas such as the tropics, species-specific models for biomass are scarce. Moreover, most models focus on large trees with a single stem. Therefore, the accuracy of these models is uncertain for estimating biomass in small and multi-stemmed trees.

This study aims to accurately estimate biomass of some tree species in Rwanda. The area is part of the second largest continuous rainforest in the world. The increase of secondary forests and the usage of young plantations in field experiments call for better biomass estimates in small trees. I sampled small trees from 8 species, including also multi-stemmed samples. I tested several equations reported by other studies by comparing their estimates to the measured biomass. I also developed new equations for each species and mixed-species equations. In addition to the often-used stem diameter at breast height, height and wood density, I included stem diameter at different heights and on several stems as well as crown area and a stem count in the models, to see if I could improve the estimates.

The results show that while some equations reported in other studies estimated the total biomass of the samples rather well, the error of estimate on individual trees were large (at least 73% of the mean biomass). Similar error was obtained by the simplest model developed for mixed species in this study. Using the diameter of the main stem at both 1.3 m and 0.3 m above ground as well as including a stem count improved the estimate in most samples. Even better was the estimate when the sum of the diameter of all stems at the lower level was used. Crown area did also improve the estimate to some extent. The best estimates were however obtained by the species-specific models, where a single diameter measurement often was enough to lower the error to under 20%. The species-specific equations presented in this study can be used to more accurately estimate the biomass of small and multi-stemmed trees of these species. The mixed-species equations could possibly be used on other species as well. The study also contributes to the understanding of variability in small trees, in particular when multi-stemmed samples occur, and which measurements are needed to be taken to accurately model their biomass.

Supplemental figures and tables

Table A1. Summary of selected models for different datasets and model categories (all models, main stem and basic models). If the same model is selected in several categories, only the simplest category is shown. S-S. is single-stemmed and M-S. is multi-stemmed.

| | | | | |
|---------------------|--|------------|------------------------|------------------------|
| All samples | | | | |
| — All models | Model. ρ . d^2 . s_{sum} .NS | AIC: 11.7 | R ² : 0.966 | $\hat{\sigma}$: 0.249 |
| | $AGB_{est} = e^{1.331 + 0.833 \ln \rho + 0.137(\ln d)^2 + 1.334 \ln \sum s_i - 0.369 \ln NS + \sigma^2/2}$ | | | |
| — Main stem | Model. ρ . d^2 .s.NS | AIC: 24 | R ² : 0.96 | $\hat{\sigma}$: 0.268 |
| | $AGB_{est} = e^{1.829 + 0.770 \ln \rho + 0.158(\ln d)^2 + 1.127 \ln s + 0.521 \ln NS + \sigma^2/2}$ | | | |
| — Basic models | Model. ρ . d^2 | AIC: 90 | R ² : 0.911 | $\hat{\sigma}$: 0.401 |
| | $AGB_{est} = e^{4.688 + 0.749 \ln \rho + 0.286(\ln d)^2 + \sigma^2/2}$ | | | |
| M-S. species | | | | |
| — All models | Model. ρ . d^2 . s_{sum}^2 | AIC: -2.64 | R ² : 0.978 | $\hat{\sigma}$: 0.218 |
| | $AGB_{est} = e^{0.1834 + 0.8873 \ln \rho + 0.0788(\ln d)^2 + 0.9278 \ln \sum s_i^2 + \sigma^2/2}$ | | | |
| — Main stem | Model. ρ . d^2 .s.NS | AIC: 21 | R ² : 0.96 | $\hat{\sigma}$: 0.289 |
| | $AGB_{est} = e^{1.241 + 0.875 \ln \rho + 0.125(\ln d)^2 + 1.436 \ln s + 0.425 \ln NS + \sigma^2/2}$ | | | |
| — Basic models | Model. ρ . d^2 | AIC: 56.4 | R ² : 0.9 | $\hat{\sigma}$: 0.461 |
| | $AGB_{est} = e^{5.164 + 1.174 \ln \rho + 0.286(\ln d)^2 + \sigma^2/2}$ | | | |
| M-S. samples | | | | |
| — All models | Model. ρ . d . s_{sum}^2 .h | AIC: 0.219 | R ² : 0.984 | $\hat{\sigma}$: 0.202 |
| | $AGB_{est} = e^{-3.869 + 0.747 \ln \rho + 0.437 \ln d + 0.911 \ln \sum s_i^2 + 0.600 \ln h + \sigma^2/2}$ | | | |
| — Main stem | Model. ρ . d .s | AIC: 17.3 | R ² : 0.95 | $\hat{\sigma}$: 0.351 |
| | $AGB_{est} = e^{-0.485 + 0.641 \ln \rho + 1.262 \ln d + 1.222 \ln s + \sigma^2/2}$ | | | |
| — Basic models | Model. d^2 . $h\rho$ | AIC: 19.9 | R ² : 0.94 | $\hat{\sigma}$: 0.399 |
| | $AGB_{est} = e^{-2.481 + 0.882 \ln d^2 h\rho + \sigma^2/2}$ | | | |
| — Basic models | Model. ρ . d^2 | AIC: -8.49 | R ² : 0.971 | $\hat{\sigma}$: 0.207 |
| | $AGB_{est} = e^{4.0609 + 0.0617 \ln \rho + 0.2868(\ln d)^2 + \sigma^2/2}$ | | | |
| S-S. samples | | | | |
| — Main stem | Model. ρ . d^2 .s.h | AIC: -6.53 | R ² : 0.971 | $\hat{\sigma}$: 0.219 |
| | $AGB_{est} = e^{4.103 + 1.014 \ln \rho + 0.196(\ln d)^2 + 1.067 \ln s - 0.393 \ln h + \sigma^2/2}$ | | | |
| — Basic models | Model. ρ . d^2 .h | AIC: 19.7 | R ² : 0.956 | $\hat{\sigma}$: 0.268 |
| | $AGB_{est} = e^{6.644 + 0.969 \ln \rho + 0.320(\ln d)^2 - 0.393 \ln h + \sigma^2/2}$ | | | |

Table A1 (continued). Summary of selected models for different datasets and model categories (all models, main stem and basic models). If the same model is selected in several categories, only the simplest category is shown. S-S. is single-stemmed and M-S. is multi-stemmed.

| | | | | |
|----------------------------|--|-------------|------------------------|-------------------------|
| B. micrantha | | | | |
| — All models | Model.d.s _{sum} ² | AIC: -1.41 | R ² : 0.969 | $\hat{\sigma}$: 0.181 |
| | $AGB_{est} = e^{-0.448 + 0.919 \ln d + 0.687 \ln \sum s_i^2 + \sigma^2/2}$ | | | |
| | | | | |
| — Basic models | Model.d ² | AIC: 6.05 | R ² : 0.938 | $\hat{\sigma}$: 0.271 |
| | $AGB_{est} = e^{5.546 + 0.241(\ln d)^2 + \sigma^2/2}$ | | | |
| C. megalocarpus | | | | |
| — Main stem | Model.d.d ² .d ³ .NS | AIC: -2.98 | R ² : 0.99 | $\hat{\sigma}$: 0.162 |
| | $AGB_{est} = e^{0.621 + 5.587 \ln d + -2.044(\ln d)^2 + 0.292(\ln d)^3 + 0.553 \ln NS + \sigma^2/2}$ | | | |
| | | | | |
| — Basic models | Model.d ² | AIC: 10.9 | R ² : 0.96 | $\hat{\sigma}$: 0.345 |
| | $AGB_{est} = e^{4.230 + 0.308(\ln d)^2 + \sigma^2/2}$ | | | |
| E. exselsum | | | | |
| — Main stem | Model.d.CA | AIC: -21 | R ² : 0.992 | $\hat{\sigma}$: 0.0679 |
| | $AGB_{est} = e^{3.880 + 2.601 \ln d + -0.511 \ln CA + \sigma^2/2}$ | | | |
| | | | | |
| — Basic models | Model.d | AIC: -9.68 | R ² : 0.976 | $\hat{\sigma}$: 0.124 |
| | $AGB_{est} = e^{0.491 + 2.020 \ln d + \sigma^2/2}$ | | | |
| M. kilimandscharica | | | | |
| — Main stem | Model.d ² .s ² .NS | AIC: -3.26 | R ² : 0.952 | $\hat{\sigma}$: 0.161 |
| | $AGB_{est} = e^{3.035 + 0.138(\ln d)^2 + 0.174(\ln s)^2 + 0.793 \ln NS + \sigma^2/2}$ | | | |
| | | | | |
| — Basic models | Model.d ² h | AIC: 21.7 | R ² : 0.413 | $\hat{\sigma}$: 0.594 |
| | $AGB_{est} = e^{-0.495 + 0.618 \ln d^2 h + \sigma^2/2}$ | | | |
| M. platycalyx | | | | |
| — Main stem | Model.s.h | AIC: -9.09 | R ² : 0.987 | $\hat{\sigma}$: 0.143 |
| | $AGB_{est} = e^{-4.367 + 1.536 \ln s + 0.984 \ln h + \sigma^2/2}$ | | | |
| | | | | |
| — Basic models | Model.d ² h | AIC: -0.764 | R ² : 0.976 | $\hat{\sigma}$: 0.203 |
| | $AGB_{est} = e^{-2.588 + 0.776 \ln d^2 h + \sigma^2/2}$ | | | |
| N. buchananii | | | | |
| — Main stem | Model.d ² .s ² .h.CA | AIC: -12.4 | R ² : 0.993 | $\hat{\sigma}$: 0.101 |
| | $AGB_{est} = e^{-3.8926 + 0.0997(\ln d)^2 + 0.1307(\ln s)^2 + 1.7880 \ln h + -0.2935 \ln CA + \sigma^2/2}$ | | | |
| | | | | |
| — Basic models | Model.d ² .h | AIC: -6.07 | R ² : 0.987 | $\hat{\sigma}$: 0.143 |
| | $AGB_{est} = e^{-5.312 + 0.177(\ln d)^2 + 1.694 \ln h + \sigma^2/2}$ | | | |

Table A1 (continued). Summary of selected models for different datasets and model categories (all models, main stem and basic models). If the same model is selected in several categories, only the simplest category is shown. S-S. is single-stemmed and M-S. is multi-stemmed.

P. falcatus

— *Main stem* **Model.s²** **AIC:** -4.49 **R²:** 0.991 **σ̂:** 0.16
 $AGB_{est} = e^{3.311 + 0.314(\ln s)^2 + \sigma^2/2}$

.....

— *Basic models* **Model.d²** **AIC:** 0.128 **R²:** 0.986 **σ̂:** 0.202
 $AGB_{est} = e^{4.251 + 0.279(\ln d)^2 + \sigma^2/2}$

P. fulva

— *All models* **Model.d².d_{sum}².CA.NS** **AIC:** -25.1 **R²:** 0.999 **σ̂:** 0.0537
 $AGB_{est} = e^{-3.6054 + 0.0733(\ln d)^2 + 0.7969 \ln \sum d_i^2 + 0.3883 \ln CA + 0.1378 \ln NS + \sigma^2/2}$

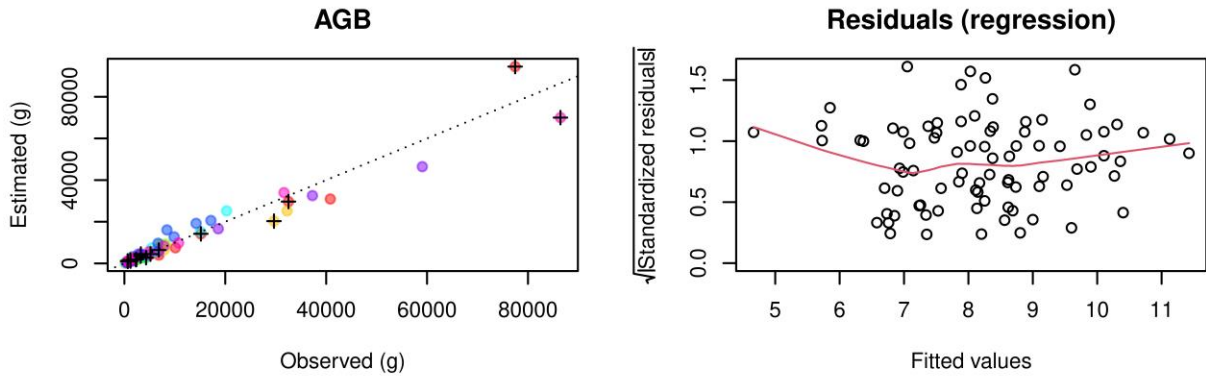
.....

— *Main stem* **Model.s².NS** **AIC:** 0.276 **R²:** 0.985 **σ̂:** 0.197
 $AGB_{est} = e^{2.202 + 0.333(\ln s)^2 + 0.554 \ln NS + \sigma^2/2}$

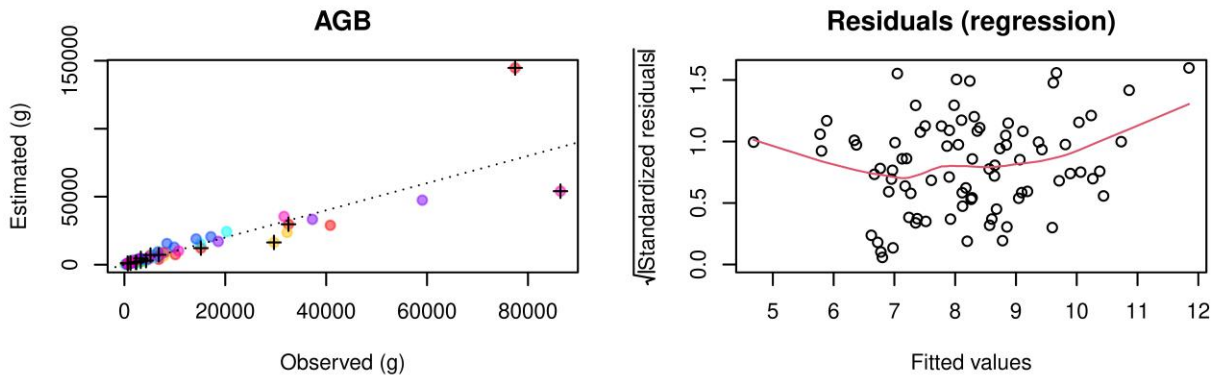
.....

— *Basic models* **Model.d²** **AIC:** 8.64 **R²:** 0.968 **σ̂:** 0.309
 $AGB_{est} = e^{3.241 + 0.314(\ln d)^2 + \sigma^2/2}$

All samples – All models



All samples – Main stem



All samples – Basic models

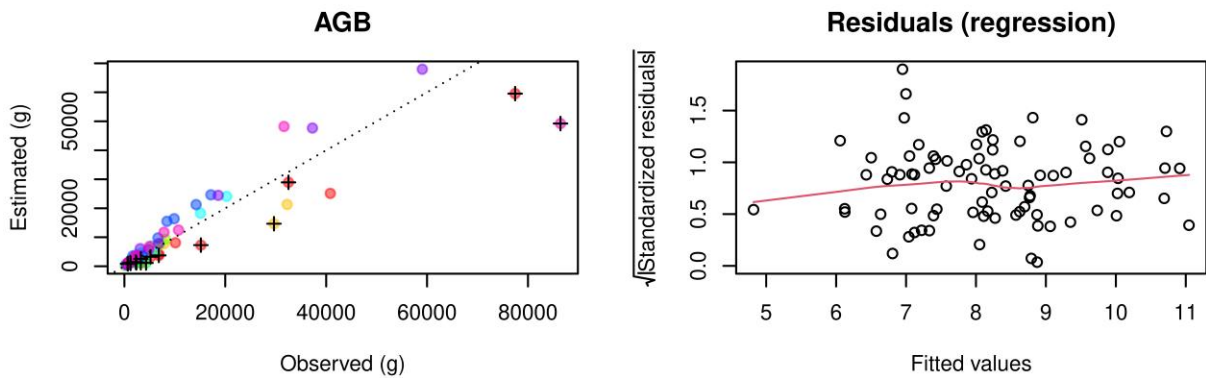
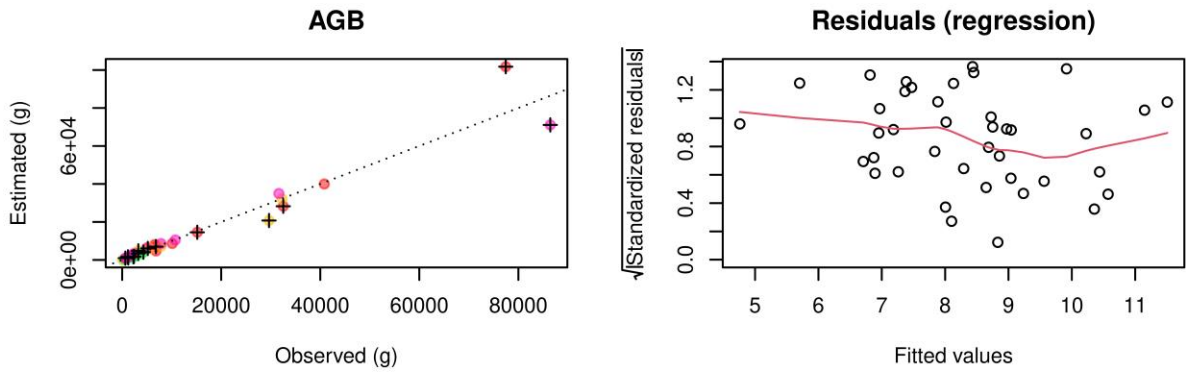
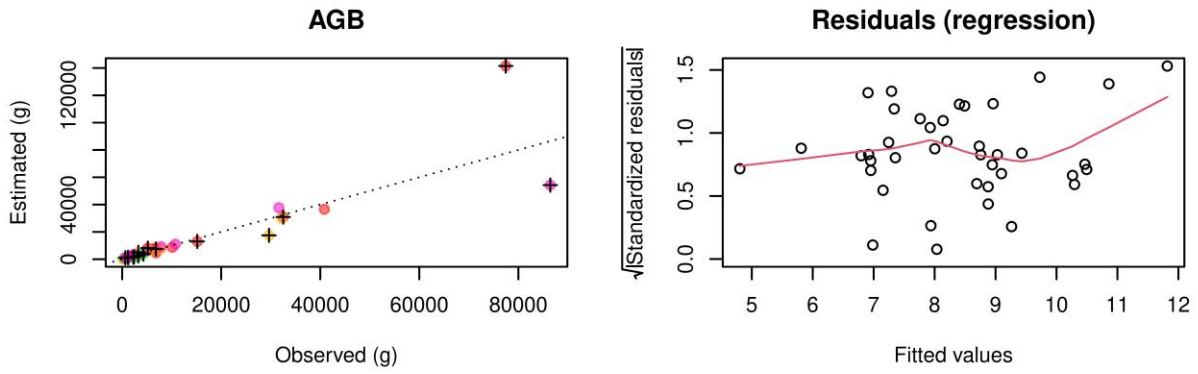


Figure A1. Plots to the left show estimated against observed AGB, for the selected models for different datasets. Model categories shown are: all models, main stem, and basic models. If the same model is selected in several categories, only the simplest category is shown. Colors indicate species and crosses mark multi-stemmed individuals. Plots to the right show regression residuals for the models, respectively.

M-S. species – All models



M-S. species – Main stem



M-S. species – Basic models

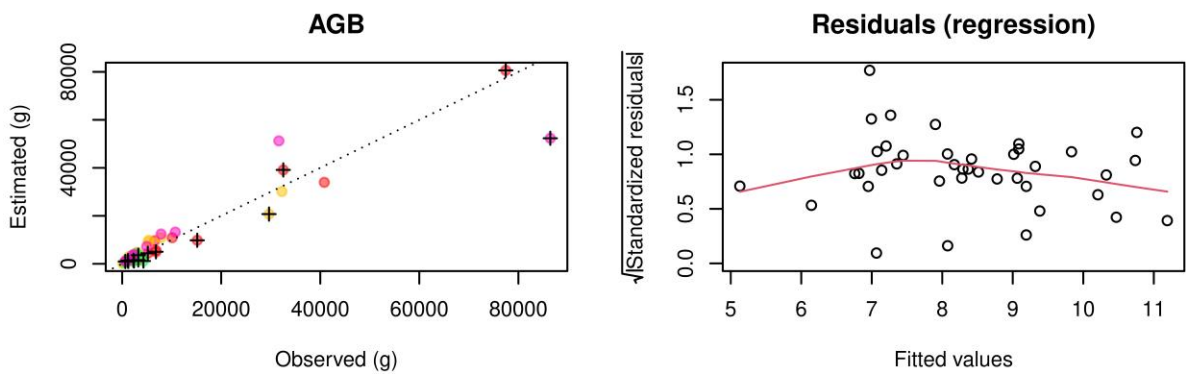
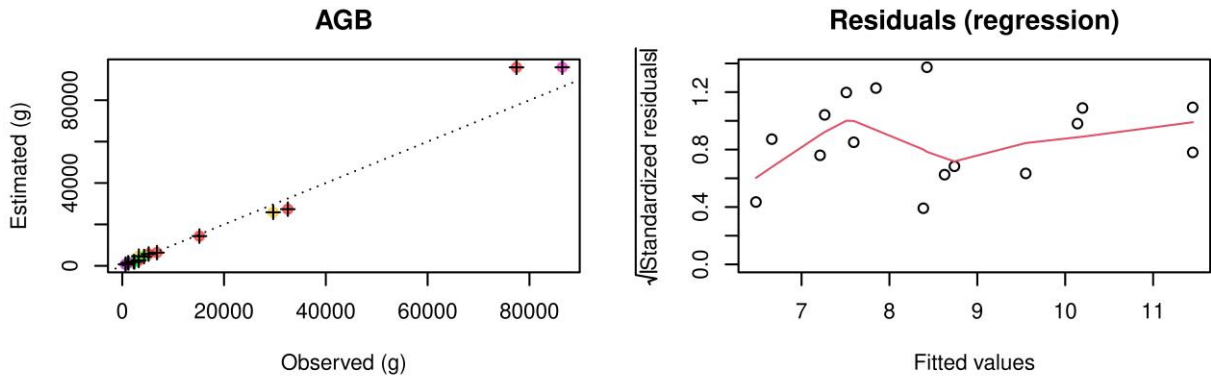
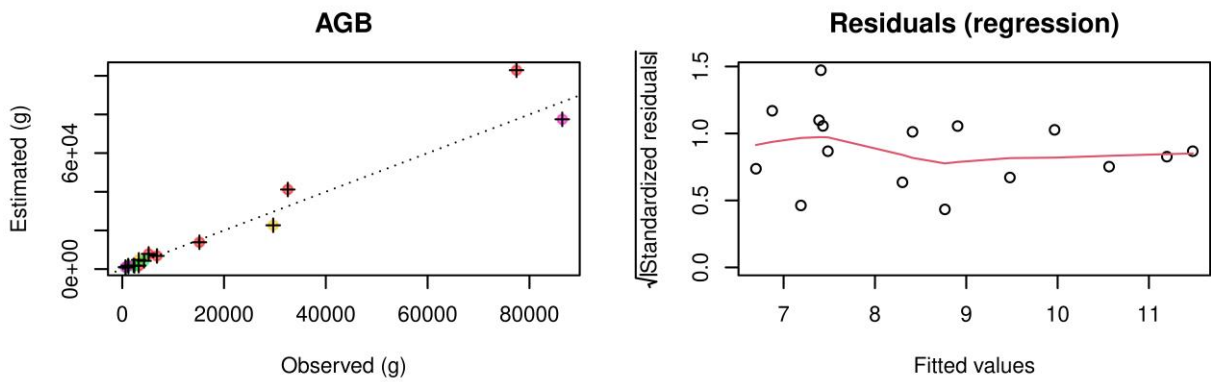


Figure A1 (continued). Plots to the left show estimated against observed AGB, for the selected models for different datasets. Model categories shown are: all models, main stem, and basic models. If the same model is selected in several categories, only the simplest category is shown. Colors indicate species and crosses mark multi-stemmed individuals. Plots to the right show regression residuals for the models, respectively.

M-S. samples - All models



M-S. samples - Main stem



M-S. samples - Basic models

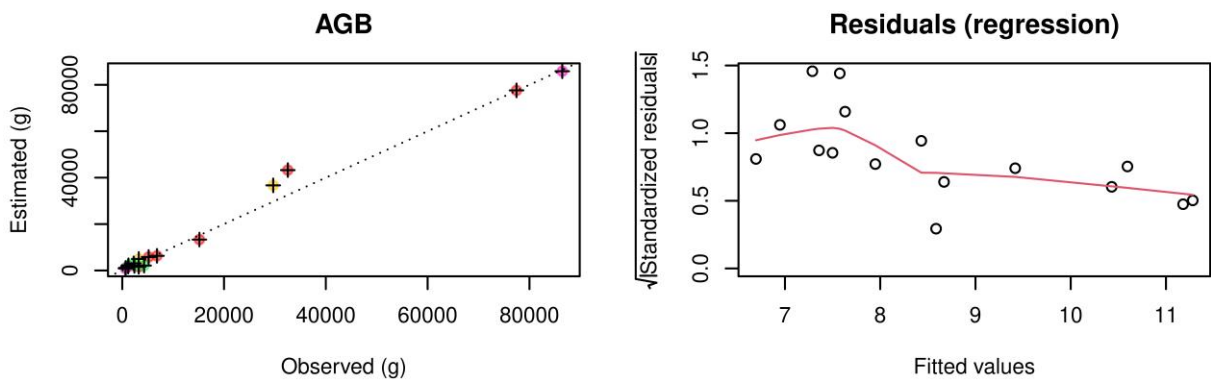
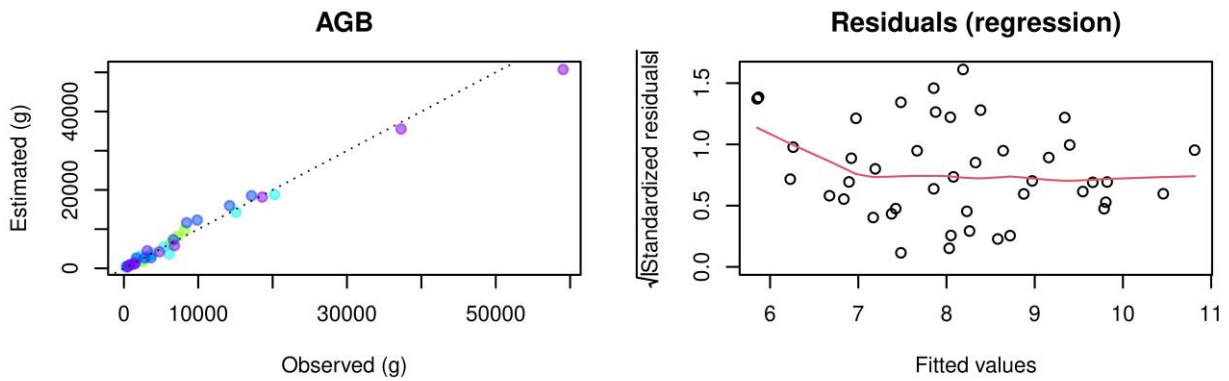
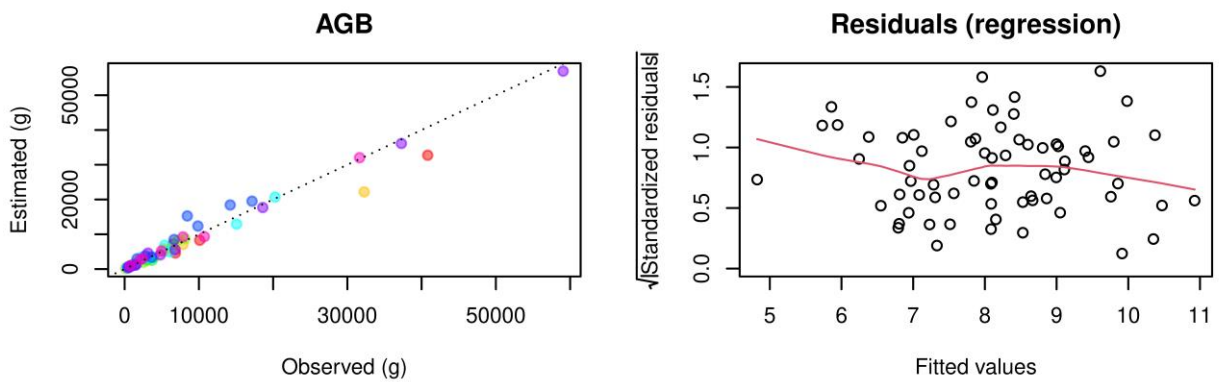


Figure A1 (continued). Plots to the left show estimated against observed AGB, for the selected models for different datasets. Model categories shown are: all models, main stem, and basic models. If the same model is selected in several categories, only the simplest category is shown. Colors indicate species and crosses mark multi-stemmed individuals. Plots to the right show regression residuals for the models, respectively.

S-S. species – Basic models



S-S. samples – Main stem



S-S. samples – Basic models

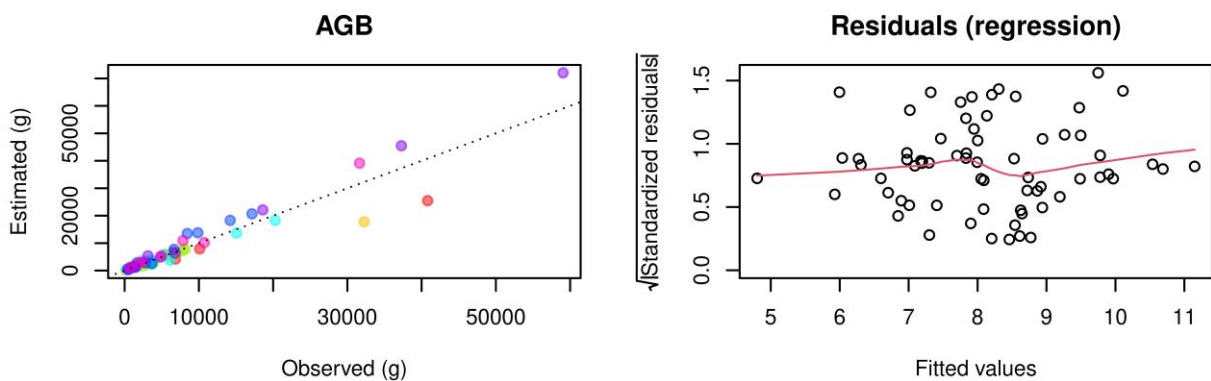
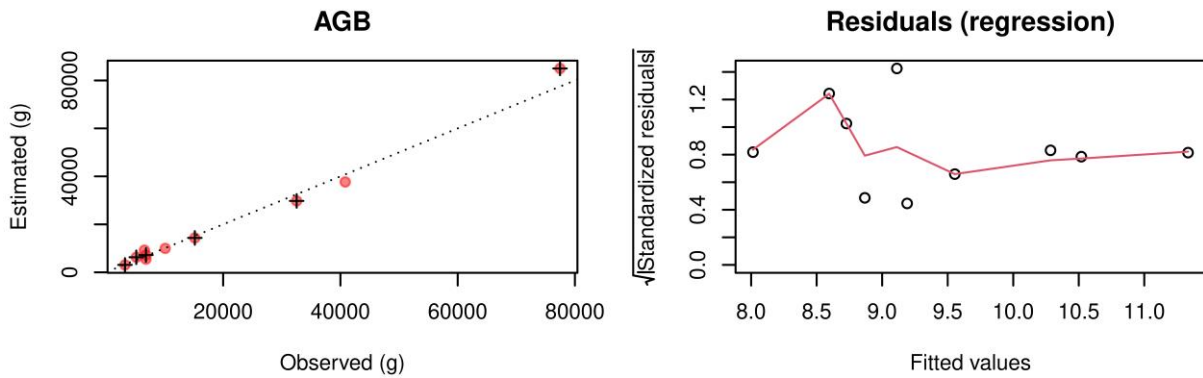
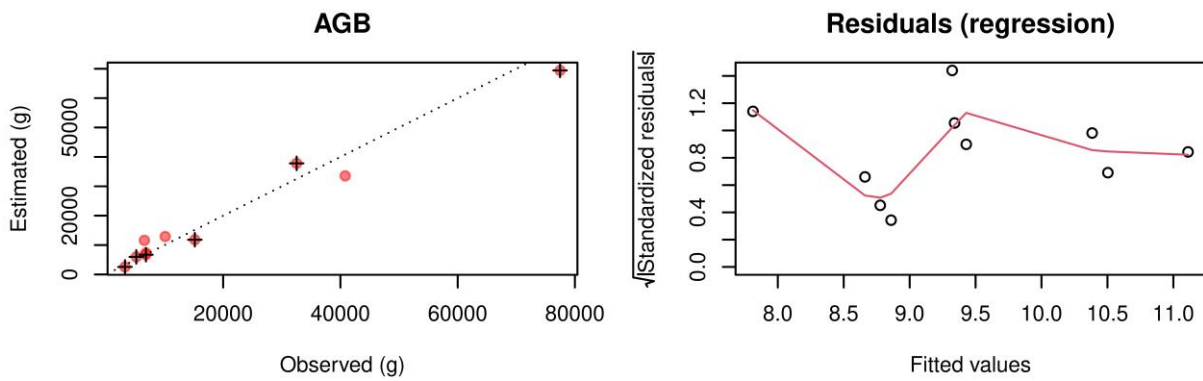


Figure A1 (continued). Plots to the left show estimated against observed AGB, for the selected models for different datasets. Model categories shown are: all models, main stem, and basic models. If the same model is selected in several categories, only the simplest category is shown. Colors indicate species and crosses mark multi-stemmed individuals. Plots to the right show regression residuals for the models, respectively.

B. micrantha – All models



B. micrantha – Basic models



C. megalocarpus – Main stem

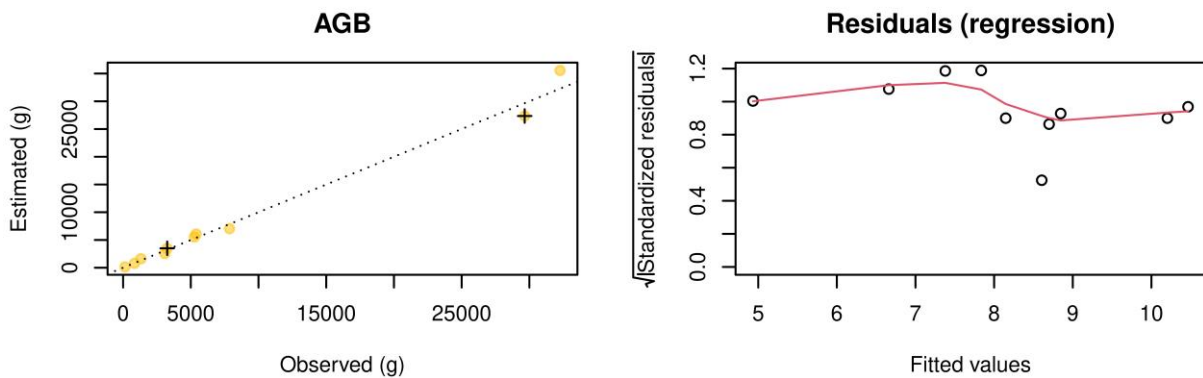
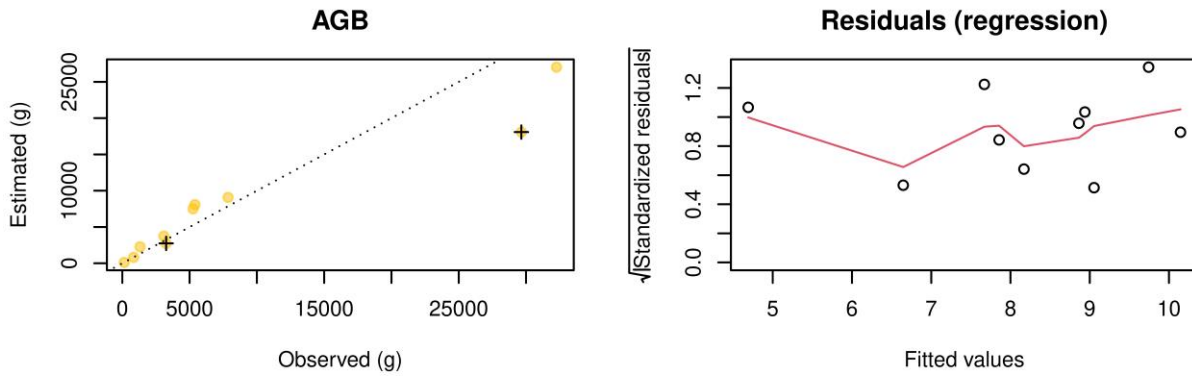
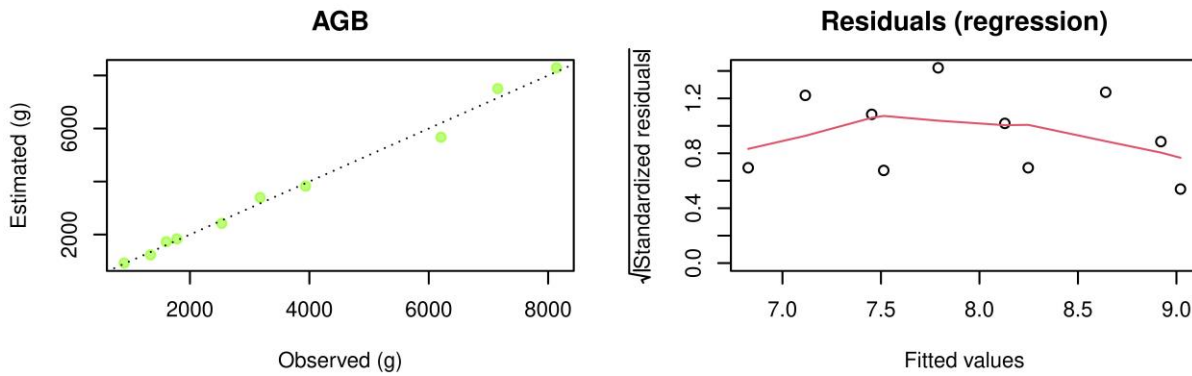


Figure A1 (continued). Plots to the left show estimated against observed AGB, for the selected models for different datasets. Model categories shown are: all models, main stem, and basic models. If the same model is selected in several categories, only the simplest category is shown. Colors indicate species and crosses mark multi-stemmed individuals. Plots to the right show regression residuals for the models, respectively.

C. megalocarpus – Basic models



E. exselsum – Main stem



E. exselsum – Basic models

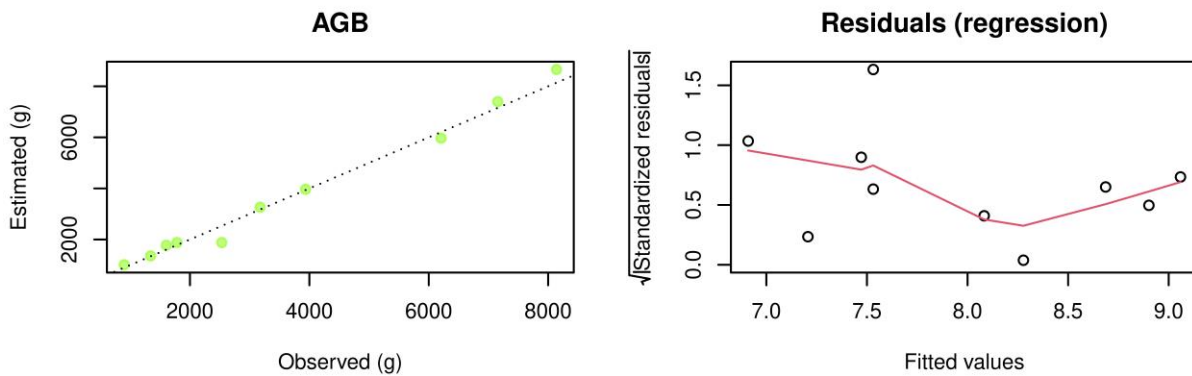
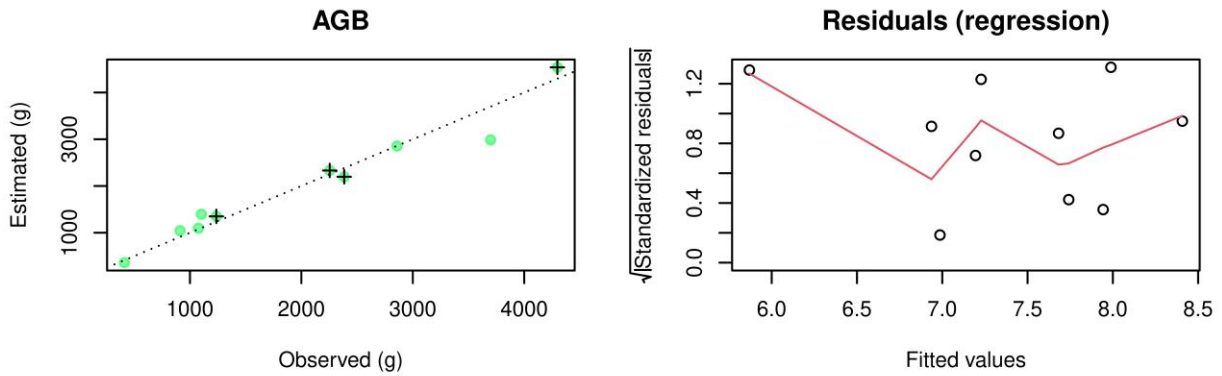
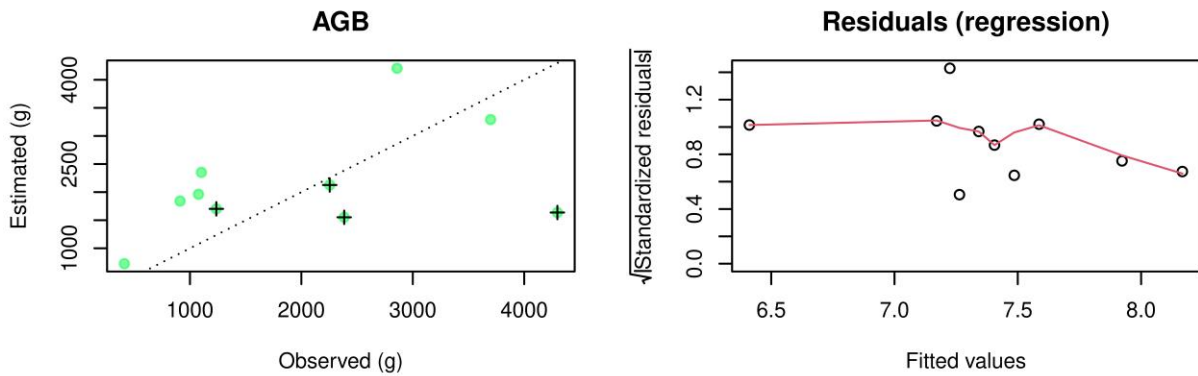


Figure A1 (continued). Plots to the left show estimated against observed AGB, for the selected models for different datasets. Model categories shown are: all models, main stem, and basic models. If the same model is selected in several categories, only the simplest category is shown. Colors indicate species and crosses mark multi-stemmed individuals. Plots to the right show regression residuals for the models, respectively.

M. kilimandscharica – Main stem



M. kilimandscharica – Basic models



M. platycalyx – Main stem

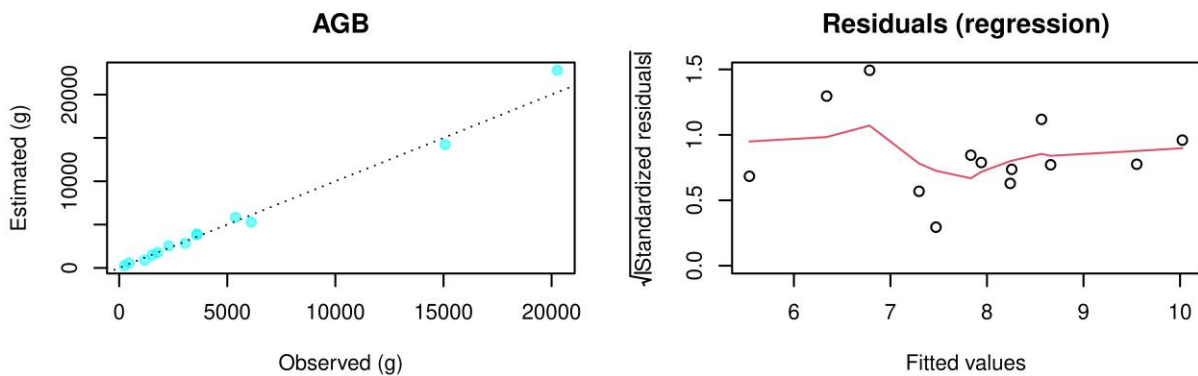
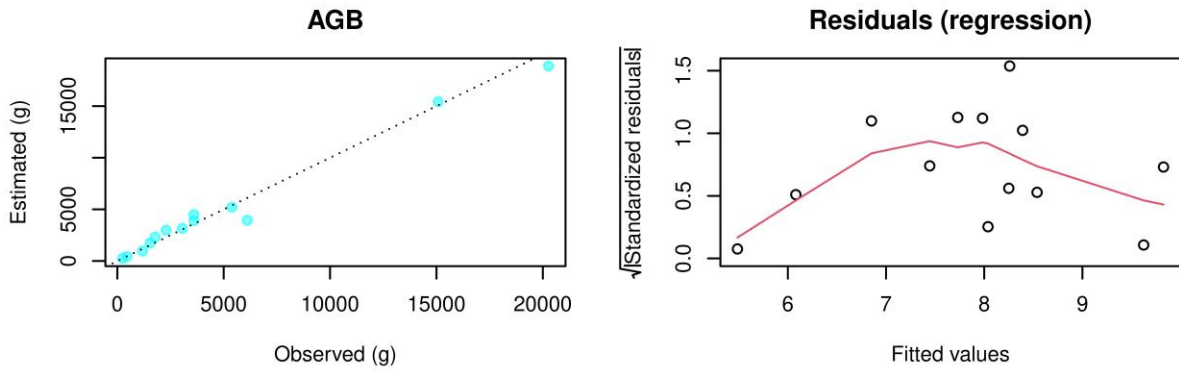
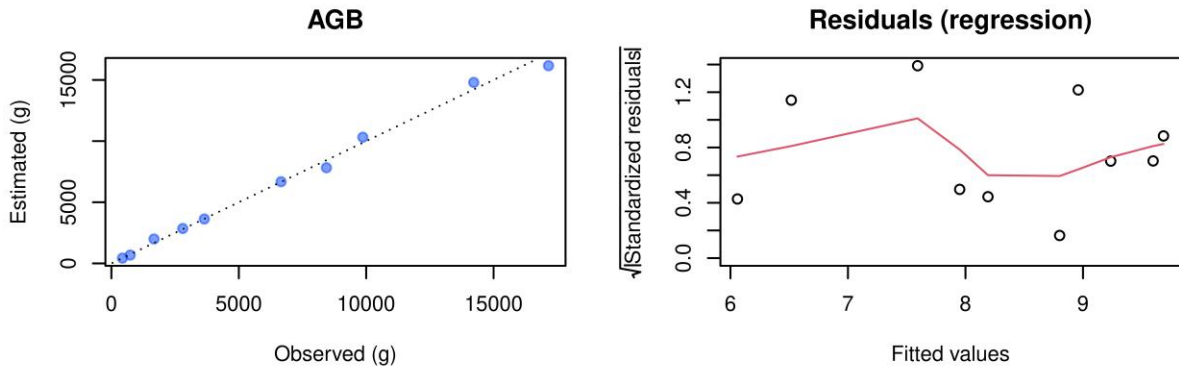


Figure A1 (continued). Plots to the left show estimated against observed AGB, for the selected models for different datasets. Model categories shown are: all models, main stem, and basic models. If the same model is selected in several categories, only the simplest category is shown. Colors indicate species and crosses mark multi-stemmed individuals. Plots to the right show regression residuals for the models, respectively.

M. platycalyx – Basic models



N. buchananii – Main stem



N. buchananii – Basic models

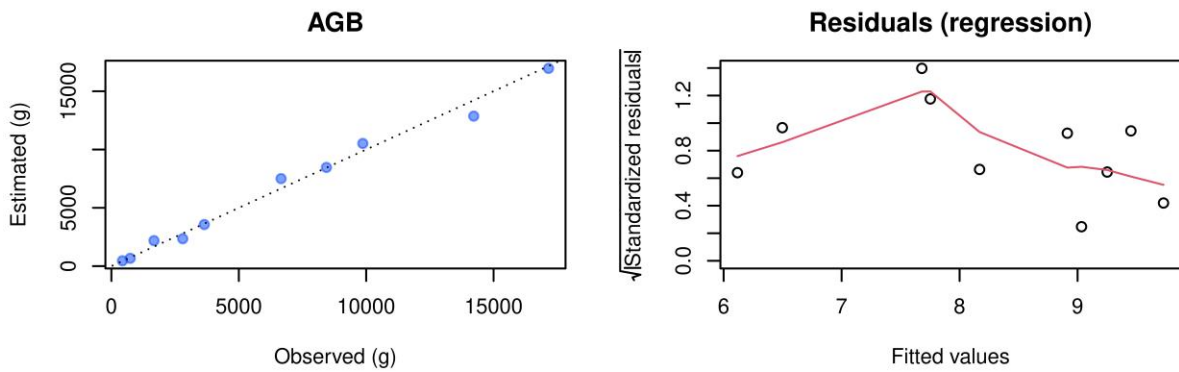
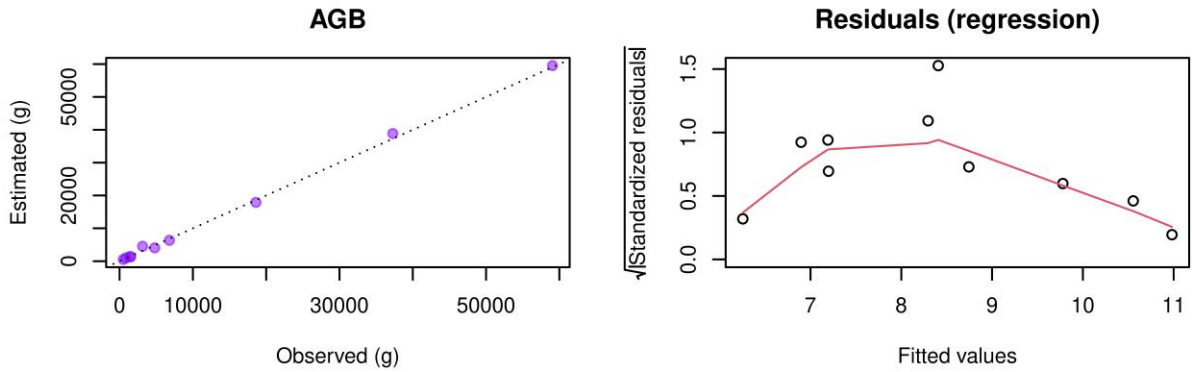
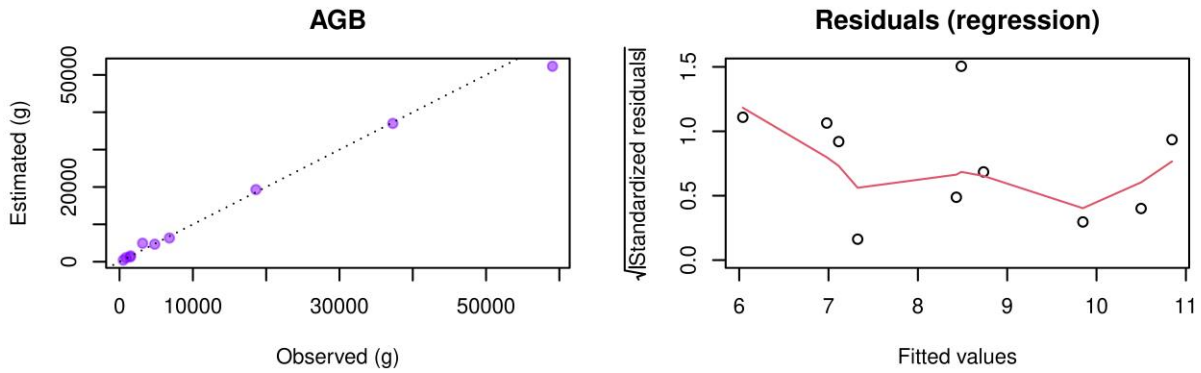


Figure A1 (continued). Plots to the left show estimated against observed AGB, for the selected models for different datasets. Model categories shown are: all models, main stem, and basic models. If the same model is selected in several categories, only the simplest category is shown. Colors indicate species and crosses mark multi-stemmed individuals. Plots to the right show regression residuals for the models, respectively.

P. falcatus – Main stem



P. falcatus – Basic models



P. fulva – All models

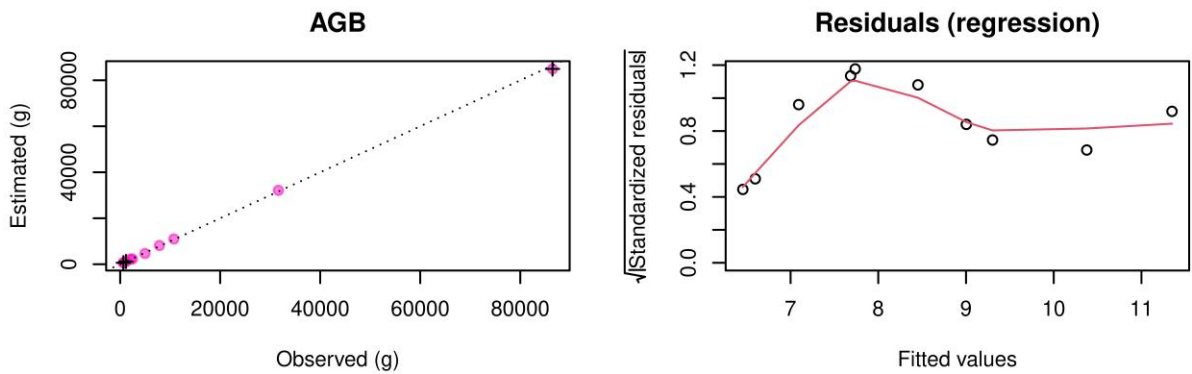
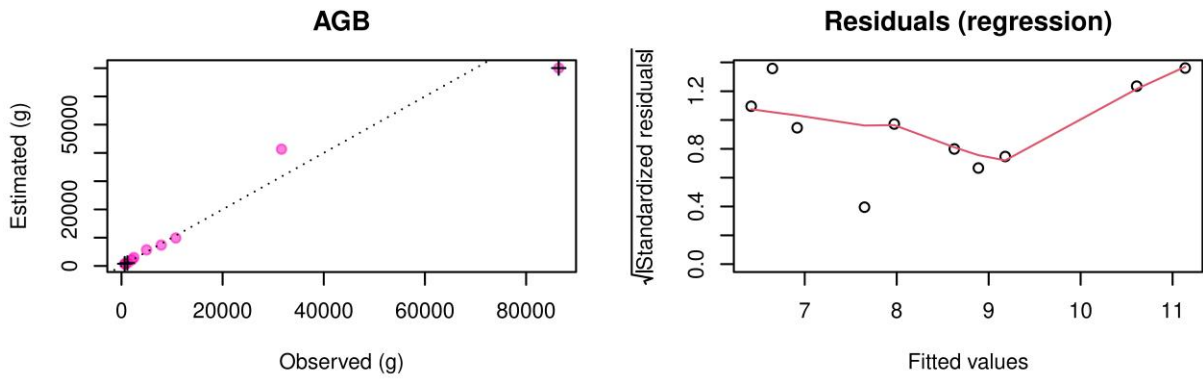


Figure A1 (continued). Plots to the left show estimated against observed AGB, for the selected models for different datasets. Model categories shown are: all models, main stem, and basic models. If the same model is selected in several categories, only the simplest category is shown. Colors indicate species and crosses mark multi-stemmed individuals. Plots to the right show regression residuals for the models, respectively.

P. fulva – Main stem



P. fulva – Basic models

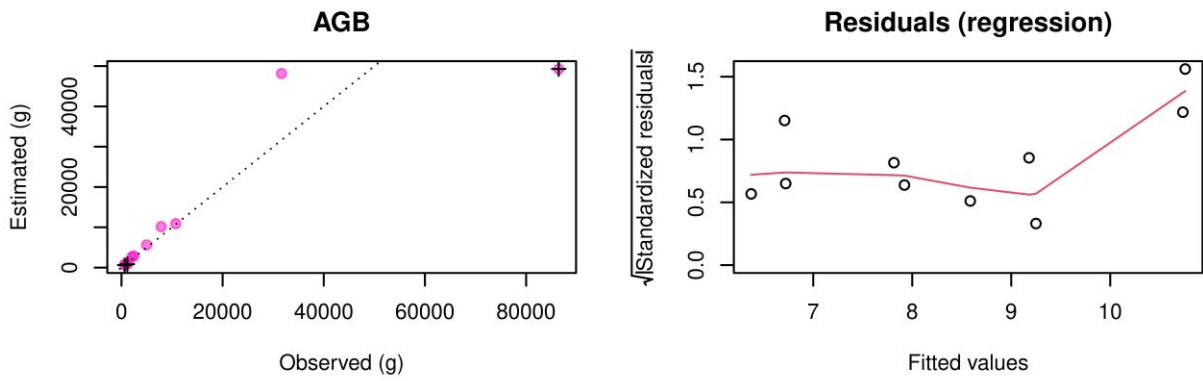


Figure A1 (continued). Plots to the left show estimated against observed AGB, for the selected models for different datasets. Model categories shown are: all models, main stem, and basic models. If the same model is selected in several categories, only the simplest category is shown. Colors indicate species and crosses mark multi-stemmed individuals. Plots to the right show regression residuals for the models, respectively.